

Confronting the IR Fixed Point Cosmology with High Redshift Observations

Eloisa Bentivegna*

*Dipartimento di Fisica e Astronomia, Università degli Studi di Catania,
Via S.Sofia 64, I-95123 Catania, Italy*

Alfio Bonanno†

*INAF, Osservatorio Astrofisico di Catania,
Via S.Sofia 78, I-95123 Catania, Italy‡*

Martin Reuter§

*Institut für Physik, Universität Mainz
Staudingerweg 7, D-55099 Mainz, Germany*

Abstract

We use high-redshift type Ia supernova and compact radio source data in order to test the infrared (IR) fixed point model of the late Universe which was proposed recently. It describes a cosmology with a time dependent cosmological constant and Newton constant whose dynamics arises from an underlying renormalization group flow near an IR-attractive fixed point. Without any finetuning or quintessence field it yields $\Omega_M = \Omega_\Lambda = 1/2$. Its characteristic $t^{4/3}$ -dependence of the scale factor leads to a distance-redshift relation whose predictions are compared both to the supernova and to the radio source data. According to the χ^2 test, the fixed point model reproduces the data at least as well as the best-fit (Friedmann-Robertson-Walker) standard cosmology. Furthermore, we extend the original fixed point model by assuming that the fixed point epoch is preceded by an era with constant G and Λ . By means of a Monte Carlo simulation we show that the data expected from the forthcoming SNAP satellite mission could detect the transition to the fixed point regime provided it took place at a redshift of less than about 0.5.

*Electronic address: ebe@ct.astro.it

†Electronic address: abo@ct.astro.it

‡Also at INFN, Sezione di Catania, Via S.Sofia 73

§Electronic address: reuter@thep.physik.uni-mainz.de

I. INTRODUCTION

In recent years renormalization group (RG) techniques have been extensively applied in cosmology, for instance in a classical averaging scenario [1] or in discussing the late-time behavior of the classical Einstein equations [2]. As for possible quantum gravitational effects, an exact functional RG equation [3] for Quantum Einstein Gravity (QEG) has been introduced [4, 5] and, within certain approximations (truncations of “theory space”), its predictions for the scale dependence of Newton’s constant G and the cosmological constant Λ have been worked out [6, 7, 8, 9].

In particular, it was found [6, 10, 11] that the ultraviolet (UV) behavior of QEG is likely to be governed by a non-Gaussian RG fixed point which would render the theory nonperturbatively renormalizable. If so, QEG is mathematically consistent and predictive at arbitrarily short distances and, in cosmology, at times arbitrarily close to the initial singularity. In ref. [12] we investigated how the standard Friedmann-Robertson-Walker (FRW) cosmology gets modified when the scale dependence of G and Λ is taken into account. We “RG improved” Einstein’s equation by replacing $G \rightarrow G(k)$, $\Lambda \rightarrow \Lambda(k)$, where k is the running mass scale which may be identified with the inverse of the cosmological time in a homogeneous and isotropic Universe, $k \propto 1/t$. In this manner the RG running gives rise to a dynamically evolving, time dependent G and Λ [13]. The improvement of Einstein’s equation can be based upon any RG trajectory $k \mapsto (G(k), \Lambda(k))$ obtained as an (approximate) solution to the exact RG equation of QEG. In particular, if the non-Gaussian UV fixed point predicted by all known solutions does indeed exist, $G(k)$ and $\Lambda(k)$ scale in a very simple manner as $k \rightarrow \infty$. In fact, the dimensionless Newton constant $g(k) \equiv k^2 G(k)$ and cosmological constant $\lambda(k) \equiv \Lambda(k)/k^2$ are attracted towards their fixed point values g_* and λ_* , respectively, and therefore, in the fixed point regime,

$$G(k) = \frac{g_*}{k^2} \tag{1a}$$

$$\Lambda(k) = \lambda_* k^2 \tag{1b}$$

In ref. [12] the improved cosmology resulting from the trajectory (1) was analyzed in detail. As the fixed point (g_*, λ_*) is approached for $k \rightarrow \infty$, it applies to the very early Universe ($t \rightarrow 0$). It turned out that the cosmology of this “Planck era” is described by an essentially unique attractor solution to the cosmological evolution equations which might provide a

solution to the horizon and flatness problems of standard cosmology without invoking an inflationary era¹.

One of the remarkable properties of the attractor solution is that it dynamically adjusts the vacuum energy density $\rho_\Lambda \equiv \Lambda/8\pi G$ so as to equal precisely the matter energy density. In units of the critical density, the spatially flat solution has

$$\Omega_\Lambda(t) = \Omega_M(t) = \frac{1}{2} \quad (2)$$

at any time during the fixed point era. This adjustment mechanism has led to the speculation [16] that not only the very early, but also the very *late* history of the Universe is described by a RG-improved Einstein equation based upon the trajectory (1). In this scenario one postulates that, in addition to the UV-attractive fixed point discussed so far, there exists a second fixed point $(g_*^{\text{IR}}, \lambda_*^{\text{IR}})$ in (g, λ) -space towards which every trajectory $k \mapsto (g(k), \lambda(k))$ within a certain basin of attraction is attracted for $k \rightarrow 0$. On very large scales the cutoff identification $k \propto 1/t$ should still be correct so that for $t \rightarrow \infty$ the IR fixed point determines the asymptotically late cosmology. The IR fixed point hypothesis implies that for $k \rightarrow 0$ or $t \rightarrow \infty$, too, G and Λ evolve accordingly to (1). (In the sequel we shall omit the superscripts “IR” from g_* and λ_* but it should be kept in mind that the values of g_* and λ_* are different at the two fixed points.) The main motivation for this hypothesis comes from the fact that, provided the Universe is spatially flat and has entered the fixed point regime already, the densities Ω_Λ and Ω_M are unambiguously predicted to assume the value 0.5. This is intriguingly close to the values $\Omega_\Lambda \approx 0.7$, $\Omega_M \approx 0.3$ favored by recent observations when interpreted within standard FRW cosmology. Hence the IR fixed point might provide a natural solution to the “cosmic coincidence problem” [17] which does not require quintessence field.

As for their actual verification within QEG, the UV and the IR fixed points have a rather different status for the time being. While the existence of the UV fixed point has actually been demonstrated within certain approximations whose reliability was tested in detail by means of rather involved calculations [6, 7], to date there is no comparable evidence for the IR fixed point. (See refs. [8, 18], however.) The technical reason is that it is extremely difficult to follow the RG flow from the UV all the way down to the IR. Therefore a $k \rightarrow 0$

¹ A similar RG improvement of black hole spacetimes can be found in refs. [14, 15].

RG-running of the form (1) has the status of a conjecture for the time being; it is motivated by its remarkable phenomenological success. We also emphasize that the RG-running of G and Λ should not necessarily be thought of as arising from quantum effects; in principle it could also result from a purely classical averaging (coarse graining) [1].

The general properties of the IR fixed point (IRFP) cosmology were first discussed in ref. [16] and will be reviewed briefly in subsection II A. In ref. [19] the theory of small perturbations about the IRFP cosmology has been developed and its consequences for the cosmological structure formation were discussed.

In the present paper we are going to test the IRFP cosmology by confronting its predictions with the currently available data on distant type Ia supernovae and compact (\sim milliarcsecond) radio sources. The relevant quantities which can be compared to the data are the luminosity distance $d_L(z)$ and the angular diameter distance $d_A(z)$, as functions of the redshift. In standard FRW cosmology these functions depend on Ω_M and Ω_Λ , and these parameters are fitted so as to reproduce the observations as well as possible. In the IRFP cosmology instead, the functions $d_L(z)$ and $d_A(z)$ contain *no free parameters* at all. Hence an acceptable fit to the data would be a rather non-trivial success of the IRFP scenario.

In particular we apply the χ^2 test to the combined dataset of 92 type Ia supernovae discovered by the Supernova Cosmology Project (SCP) [22] and the High- z Supernova Search Team (HzST) [23] and to the radio source data set of [28]. As far as the χ^2 test is concerned, we shall show that the IRFP cosmology has a reduced χ^2 value which is basically the same as that of the best-fit FRW solution. In the Appendix, we also apply the median statistics analysis [20, 21] to the SNe Ia fit, and then use the Bayesian approach to test the robustness of the hypothesis that the correct model of the late Universe is the IRFP cosmology, and we show that the posterior probability that the late Universe is described by the IRFP cosmology is 36%. The corresponding probability for the best-fit FRW cosmology is only 24%. These numbers are obtained from a specific choice of the priors which was used in the literature already earlier, but of course, as always, it contains a certain degree of arbitrariness.

The rest of this paper is organized as follows. In Section II we discuss the basic properties of the IRFP cosmology and introduce a possible extension of the model which describes the complete transition from a preceding FRW era to the IRFP cosmology. Section III is devoted to the calculation of the luminosity distance, and to the data analysis by means of the χ^2 test. In Section IV we perform an analogous cosmological test, based on the angular diameter

distance-redshift relation. In Section V we discuss arbitrary power law cosmologies with variable G and Λ which generalize the IRFP model. In Section VI we derive a constraint on the IRFP from the CMBR acoustic peaks, and Section VII is devoted to the conclusions.

II. THE MODEL

A. The fixed point cosmology

In this subsection we shall review the basic properties of the IRFP cosmology. It assumes spacetime to be homogeneous and isotropic so that it can be described by a standard Robertson-Walker metric containing the scale factor $a(t)$ and the parameter $K = 0, \pm 1$ which distinguishes the three types of maximally symmetric 3-spaces of constant cosmological time t . The time evolution is governed by Einstein's equation $R_{\mu\nu} - \frac{1}{2}g_{\mu\nu}R = -\Lambda g_{\mu\nu} + 8\pi G T_{\mu\nu}$ with the conserved energy-momentum tensor $T_{\mu}{}^{\nu} = \text{diag}(-\rho, p, p, p)$. The equation of state is assumed to be of the form $p(t) = w\rho(t)$, with $w > -1$ an arbitrary constant. Now we "RG improve" Einstein's equation by replacing $G \rightarrow G(t)$ and $\Lambda \rightarrow \Lambda(t)$ which leads to the following coupled system of evolution equations [12, 16]:

$$\left(\frac{\dot{a}}{a}\right)^2 + \frac{K}{a^2} = \frac{1}{3}\Lambda + \frac{8\pi}{3}G\rho \quad (3a)$$

$$\dot{\rho} + 3(1+w)\frac{\dot{a}}{a}\rho = 0 \quad (3b)$$

$$\dot{\Lambda} + 8\pi\rho\dot{G} = 0 \quad (3c)$$

$$G(t) \equiv G(k = k(t)), \quad \Lambda(t) \equiv \Lambda(k = k(t)) \quad (3d)$$

Eq. (3a) is the familiar Friedmann equation with a time dependent G and Λ , and eq. (3b) expresses the conservation of $T_{\mu\nu}$. Eq. (3c) is a novel integrability condition which ensures that the RHS of Einstein's equation has vanishing covariant divergence.

The equations (3d) express the fact that the *time* dependence of G and Λ is the consequence of a more fundamental *scale* dependence of these quantities. We describe physics at a typical distance scale $\ell \equiv k^{-1}$ by means of a scale dependent gravitational action $\Gamma_k[g_{\mu\nu}]$ which should be thought of as a coarse grained free energy functional in the sense of Wilson. It encapsulates the effect of all metric fluctuations with momenta larger than the IR cutoff scale k , while those with smaller momenta are not yet "integrated out". In very general

terms, Γ_k describes the dynamics of fields “averaged” over spacetime volumes of linear extension k^{-1} . The k -dependence of Γ_k is governed by an exact RG equation whose precise nature is not important here. The quantum mechanical flow equation for the exact average action of QEG [4] would be one example, the classical equations of ref. [1] are another. Generically Γ_k is an arbitrary diffeomorphism-invariant functional depending on infinitely many generalized coupling constants which multiply all possible invariants which can be constructed from $g_{\mu\nu}$. We assume that we are in a regime where only the Einstein-Hilbert invariants $\int d^4x \sqrt{-g} R$ and $\int d^4x \sqrt{-g}$ are important so that the only running couplings retained are their coefficients $G(k)$ and $\Lambda(k)$. If Γ_k is of the Einstein-Hilbert form, the effective, i.e. scale dependent field equations look like the conventional Einstein equation with the replacement $G \rightarrow G(k)$, $\Lambda \rightarrow \Lambda(k)$, where $k \mapsto (G(k), \Lambda(k))$ is an approximate solution to the RG equation.

The final step of the improvement program consists in converting the k -dependence of G and Λ to a time dependence. In ref. [12] we discussed in detail that in a Robertson-Walker spacetime, to leading order, the IR cutoff should be identified as

$$k(t) = \frac{\xi}{t} \quad (4)$$

where ξ is a positive constant.

Before discussing the solutions of the system (3) some definitions are convenient. We define the vacuum energy density ρ_Λ , the total energy density ρ_{tot} and the critical energy density ρ_{crit} according to

$$\rho_\Lambda(t) \equiv \frac{\Lambda(t)}{8\pi G(t)}, \quad \rho_{\text{tot}}(t) \equiv \rho + \rho_\Lambda, \quad (5)$$

$$\rho_{\text{crit}}(t) \equiv \frac{3}{8\pi G(t)} \left(\frac{\dot{a}}{a} \right)^2 \quad (6)$$

with $H \equiv \dot{a}/a$. Hence we may rewrite the improved Friedmann equation (3a) in the form

$$\frac{\dot{a}^2 + K}{a^2} = \frac{8\pi}{3} G(t) \rho_{\text{tot}} \quad (7)$$

Frequently we refer the various energy densities to the critical density (6):

$$\Omega_M \equiv \frac{\rho}{\rho_{\text{crit}}}, \quad \Omega_\Lambda \equiv \frac{\rho_\Lambda}{\rho_{\text{crit}}}, \quad \Omega_{\text{tot}} \equiv \Omega_M + \Omega_\Lambda \equiv \frac{\rho_{\text{tot}}}{\rho_{\text{crit}}} \quad (8)$$

Another convenient abbreviation is $\Omega_K \equiv 1 - \Omega_{\text{tot}} = 1 - \Omega_M - \Omega_\Lambda$. It follows from these definitions that

$$\Lambda(t) = 3 \Omega_\Lambda(t) H^2(t) \quad (9)$$

and the Friedmann equation (7) becomes

$$K = \dot{a}^2 [\Omega_{\text{tot}} - 1] = -\dot{a}^2 \Omega_K \quad (10)$$

For a spatially flat universe ($K = 0$) we need $\rho_{\text{tot}} = \rho_{\text{crit}}$, as in standard cosmology. In this case the definition (6) entails

$$\rho_{\text{tot}}(t) G(t) H^2(t) = \frac{3}{8\pi} \quad (K = 0) \quad (11)$$

It is important to recall from [16] that the standard experimental value of Newton's constant, G_{exp} , does not coincide with the value $G(k = \xi/t_0)$ which is relevant for cosmology today, i.e. for $t = t_0$. In fact, G_{exp} is measured (today) at $k_{\text{exp}} = \xi/\ell$, where ℓ is a typical laboratory or solar system length scale. Thus, in terms of the running Newton constant, $G_{\text{exp}} = G(k = k_{\text{exp}})$, since $1/\ell \gg 1/t_0$, and since in presence of several scales the relevant cutoff is always the larger one. On the basis of the antiscreening character of gravity [4] we might expect that $G(t_0) > G_{\text{exp}}$ therefore.

Note that the critical density (6) is defined in terms of the *cosmological* Newton constant $G(t)$. In particular in order to parametrize matter densities ρ obtained by non-cosmological measurements, it is sometimes more convenient to refer ρ to a modified ‘‘critical’’ density defined in terms of the *experimental* value G_{exp} :

$$\rho_{\text{crit}}^{\text{exp}}(t) \equiv \frac{3H^2(t)}{8\pi G_{\text{exp}}} \quad (12)$$

A spatially flat universe requires $\rho_{\text{tot}} = \rho_{\text{crit}}$, but ρ_{tot} might well be different from $\rho_{\text{crit}}^{\text{exp}}$. For the relative matter density referring to $\rho_{\text{crit}}^{\text{exp}}$ we write

$$\Omega_{\text{M}}^{\text{exp}}(t) \equiv \frac{\rho(t)}{\rho_{\text{crit}}^{\text{exp}}} \quad (13)$$

This definition implies that $\Omega_{\text{M}}^{\text{exp}} = \Omega_{\text{M}} G_{\text{exp}}/G(t)$ or

$$G(t) = \frac{\Omega_{\text{M}}(t)}{\Omega_{\text{M}}^{\text{exp}}(t)} G_{\text{exp}} \quad (14)$$

In [16] we investigated the consequences of the conjecture that, for $k \rightarrow 0$, the RG trajectory for the dimensionless Newton constant $g(k) \equiv k^2 G(k)$ and cosmological constant $\lambda(k) \equiv \Lambda(k)/k^2$ runs into an infrared attractive fixed point (g_*, λ_*) with $g_* > 0$ and $\lambda_* > 0$. This means that the corresponding dimensionful quantities behave as $G(k) = g_*/k^2$, $\Lambda(k) = \lambda_* k^2$ for $k \rightarrow 0$. In the fixed point regime, the coupled system (3) for $K = 0$ and with

$k(t) = \xi/t$ was found to have an essentially unique attractor solution which governs the cosmology for $t \rightarrow \infty$:

$$a(t) = \left[\left(\frac{3}{8} \right)^2 (1+w)^4 g_* \lambda_* \mathcal{M} \right]^{1/(3+3w)} t^{4/(3+3w)} \quad (15a)$$

$$\rho(t) = \frac{8}{9\pi(1+w)^4 g_* \lambda_*} \frac{1}{t^4} \quad (15b)$$

$$G(t) = \frac{3}{8} (1+w)^2 g_* \lambda_* t^2 \quad (15c)$$

$$\Lambda(t) = \frac{8}{3(1+w)^2} \frac{1}{t^2} \quad (15d)$$

Here the conserved quantity

$$\mathcal{M} \equiv 8\pi\rho(t)[a(t)]^{3+3w} = \text{const} \quad (16)$$

is the only free constant of integration. The system (3) also fixes the parameter ξ :

$$\xi^2 = \frac{8}{3(1+w)^2 \lambda_*} \quad (17)$$

The cosmology (15) yields $\rho = \rho_\Lambda = \rho_{\text{crit}}/2$, $\rho_{\text{tot}} = \rho_{\text{crit}}$, or

$$\Omega_M = \Omega_\Lambda = \frac{1}{2}, \quad \Omega_{\text{tot}} = 1 \quad (18)$$

It is one of the most attractive consequences of the fixed point hypothesis that it leads unambiguously to these values of the relative densities. They are intriguingly close to, but not identical with, the values favored by the analyses of the recent observations within standard cosmology. We shall come back to this point later.

The Hubble parameter of the cosmology (15) is

$$H(t) = \frac{4}{3+3w} \frac{1}{t}, \quad (19)$$

and the deceleration parameter reads

$$q \equiv -\frac{a\ddot{a}}{\dot{a}^2} = \frac{3w-1}{4} \quad (20)$$

We can use (19) in order to compute the age of the Universe, t_0 , in terms of the present Hubble constant $H(t_0) \equiv H_0$:

$$t_0 = \frac{4H_0^{-1}}{3+3w} \quad (21)$$

Clearly, for the late universe, the most plausible equation of state is $p = 0$, i.e. $w = 0$. In this case the fixed point solution describes an accelerated expansion $a \propto t^{4/3}$ with the deceleration parameter $q = -1/4$ [24]. For the age of the Universe we obtain $t_0 = \frac{4}{3}H_0^{-1}$. This is precisely twice the age one would obtain in standard cosmology with $\Lambda = 0$ for the same value of H_0 .

B. Measuring $G(t_0)$ and $g_*\lambda_*$

In the sequel we assume that the present Universe is described by the fixed point solution for $K = 0$, eqs. (15), and that this fixed point behavior started at a certain transition time $t_{\text{tr}} < t_0$. Later on we shall determine t_{tr} by postulating a plausible form of the RG trajectory running into the fixed point.

In this section we discuss how, at least in principle, one can determine the present cosmological Newton constant $G(t_0)$ and the product $g_*\lambda_*$ which characterizes the fixed point. Note that the attractor solution (15) depends only on this product but not on g_* and λ_* separately. The experience with the *ultraviolet* fixed point of QEG [6, 7] suggests that the product $g_*\lambda_*$ should be scheme independent (universal) while the factors g_* and λ_* are not.

Since the fixed point solution satisfies $\rho(t) = \rho_{\text{tot}}/2$, we can use (11) in order to express $G(t_0)$ in terms of observable quantities:

$$G(t_0) = \frac{3}{16\pi} \frac{H_0^2}{\rho(t_0)} \quad (22)$$

By a very precise measurement of the Hubble constant and the matter energy density we can, in principle, determine $G(t_0)$ and compare it to the laboratory value G_{exp} . It is clear, however, that before we can check whether $G(t_0) \neq G_{\text{exp}}$, the experimental situation must improve considerably. (Note also that the RHS of (22) differs only by a factor of 2 from what one obtains in standard cosmology with $\Lambda = 0$, $K = 0$; in this case the prefactor is $3/8\pi$.)

Because $\Omega_M(t) = 1/2$ holds throughout the fixed point regime, we can interpret a deviation of $G(t_0)$ from G_{exp} also in terms of a $\Omega_M^{\text{exp}}(t_0)$ -value which differs from 1/2. From (14) we obtain

$$G(t_0) = \frac{G_{\text{exp}}}{2 \Omega_M^{\text{exp}}(t_0)} \quad (23)$$

In order to get a first idea about the ratio $G(t_0)/G_{\text{exp}}$ we consider the hypothetical extreme case in which there exists no dark matter at all. Within the standard theory, the density of known forms of matter yields roughly

$$\Omega_{\text{M}}^{\text{exp}}(t_0) \gtrsim \frac{1}{100} \quad (24)$$

Interpreting this figure within our model we find that $G(t_0)/G_{\text{exp}} \lesssim 50$. Note that the ratio $G(t_0)/G_{\text{exp}}$ cannot be many orders of magnitude larger than unity precisely because the present density is so close to the critical one.

As for the determination of $g_*\lambda_*$, we start from the relation

$$g_*\lambda_* = G(k)\Lambda(k) = G(t)\Lambda(t) = \text{const} \quad (25)$$

which, in the fixed point regime, holds for any cutoff identification $k = k(t)$. Thus, $g_*\lambda_* = G(t_0)\Lambda(t_0)$ where we may substitute

$$\Lambda(t_0) = \frac{3}{2} H_0^2 \quad (26)$$

which follows from (9) with $\Omega_{\Lambda}(t_0) = 1/2$. Therefore we can express $g_*\lambda_*$ in terms of observable quantities either as

$$g_*\lambda_* = \frac{3}{2} G(t_0) H_0^2 \quad (27)$$

or as

$$g_*\lambda_* = \frac{9}{32\pi} \frac{H_0^4}{\rho(t_0)} \quad (28)$$

We see that we can determine $g_*\lambda_*$ by measuring H_0 and $G(t_0)$ or $\rho(t_0)$, respectively. Let us introduce the Hubble length $\ell_{\text{H}}(t) \equiv 1/H(t)$ and the Planck length $\ell_{\text{Pl}} = \sqrt{G_{\text{exp}}}$, defined in the usual way in terms of the laboratory value of Newton's constant. In terms of these length scales (27) can be rewritten as

$$g_*\lambda_* = \frac{3}{2} \frac{G(t_0)}{G_{\text{exp}}} \left(\frac{\ell_{\text{Pl}}}{\ell_{\text{H}}(t_0)} \right)^2 \quad (29)$$

Since $\ell_{\text{Pl}}/\ell_{\text{H}}(t_0) = O(10^{-60})$ the product $g_*\lambda_*$ is of the order $[G(t_0)/G_{\text{exp}}] 10^{-120}$. Most probably $G(t_0)$ and G_{exp} do not differ by many orders of magnitude so that, roughly, $g_*\lambda_* = O(10^{-120})$.

We emphasize that in our scenario the smallness of this number does not pose any finetuning problem as it does in standard cosmology. In fact, $g_*\lambda_*$ is a fixed and universally defined

number which in principle can be computed from the RG equation. However, apart from being a difficult technical problem, this computation is possible only if we know the complete system of matter fields in the Universe. The number 10^{-120} reflects specific properties of this matter system coupled to gravity rather than an initial condition.

C. A natural extension of the model

Up to this point, our entire discussion was based upon the single hypothesis that, for $k \rightarrow 0$, the dimensionless couplings $g(k)$ and $\lambda(k)$ are attracted towards a fixed point (g_*, λ_*) at $g_* > 0$ and $\lambda_* > 0$. By virtue of the system (3) this information is sufficient in order to determine the cosmological evolution for $t \rightarrow \infty$. In the $K = 0$ - sector it was found to be given by the attractor solution (15). With this restricted knowledge about the RG trajectory, it is clearly impossible to determine how the Universe evolved towards the attractor, or to answer the question when the fixed point behavior set in.

In order to have a model which applies also before the transition to the fixed point era we shall now generalize our hypothesis about the RG trajectory in a very “minimal”, in fact the simplest possible way. We shall assume that the fixed point era of the cosmological evolution is preceded by an era during which G and Λ are approximately constant.

To be precise, our first hypothesis is that the relevant RG trajectory, at least at a qualitative level, can be approximated by²

$$G(k) = \begin{cases} g_*/k^2 & \text{for } k < k_{\text{tr}} \\ G_{<} & \text{for } k > k_{\text{tr}} \end{cases} \quad (30)$$

$$\Lambda(k) = \begin{cases} \lambda_* k^2 & \text{for } k < k_{\text{tr}} \\ \Lambda_{<} & \text{for } k > k_{\text{tr}} \end{cases} \quad (31)$$

We fix the constant values $G_{<}$ and $\Lambda_{<}$ in terms of the “transition scale” k_{tr} according to

$$G_{<} = \frac{g_*}{k_{\text{tr}}^2} \quad (32)$$

$$\Lambda_{<} = \lambda_* k_{\text{tr}}^2 \quad (33)$$

² Eqs. (30), (31) could, for instance, be regarded as a model for the final part of a possible crossover from the UV to the IR fixed point, similar to what happens in 2D gravity [25].

This guarantees that $G(k)$ and $\Lambda(k)$ are continuous (but not differentiable) at the transition point. Clearly a more realistic RG trajectory would be differentiable, and the transition from the regime with $G, \Lambda = \text{const}$ to the fixed point regime would occur smoothly during a finite interval Δk_{tr} centered about k_{tr} . The trajectory (30), (31) should always be understood as an idealization of a smooth RG trajectory interpolating between $G, \Lambda = \text{const}$ and the fixed point running.

Our second hypothesis concerns the identification of the cutoff in terms of dynamical variables which in general could be of the form $k = k(t, a(t), \dot{a}(t), \dots)$. Guided by the discussion in [16] we assume that the identification $k = \xi/t$, $\xi > 0$, is valid for all $k < k_{\text{tr}}$, where $t_{\text{tr}} = \xi/k_{\text{tr}}$ denotes the time at which the transition occurs. (As we shall see, the scale k_{tr} or the transition time t_{tr} are not input parameters but rather are predicted by the model itself.)

It is easy to solve the coupled system (3) for $t > t_{\text{tr}}$ and $t < t_{\text{tr}}$, respectively. For $t > t_{\text{tr}}$, the most general solution is the one parameter family of attractor solutions (15), with \mathcal{M} being the only free parameter. For $t < t_{\text{tr}}$, the unique solution (with $a(0) = 0$) is the standard spatially flat FRW cosmology with a cosmological constant $\Lambda_{<} > 0$. Its scale factor reads [12]

$$a(t) = \left[\frac{\mathcal{M}G_{<}}{2\Lambda_{<}} \left\{ \cosh \left[(1+w)\sqrt{3\Lambda_{<}} t \right] - 1 \right\} \right]^{1/(3+3w)} \quad (34)$$

and the matter density is

$$\rho(t) = \frac{\mathcal{M}}{8\pi[a(t)]^{3+3w}} \quad (35)$$

Note that the parameter \mathcal{M} has the same value in both branches of the solution because it is related to a constant of motion of the system (3) by eq. (16).

As we discussed in detail in [12], the very existence of solutions to the improved evolution equations (3) is a nontrivial issue because for a given RG trajectory and cutoff identification this system is overdetermined. While in the case at hand it is very easy to solve the equations for $t < t_{\text{tr}}$ and $t > t_{\text{tr}}$ separately, it is by no means guaranteed that, at $t = t_{\text{tr}}$, the two solutions match in a physically acceptable way. Basically we are trying to adjust *one* parameter, t_{tr} , in such a way that *four* functions, $a(t), \rho(t), G(t), \Lambda(t)$ become continuous at t_{tr} .

It is important here that in reality the transition from the classical FRW regime to the fixed point regime does not take place instantaneously, but during a finite interval of time,

Δt_{tr} , which is centered about t_{tr} . This transition period reflects the fact that the true RG trajectory is differentiable, and that there is a smooth transition from $G, \Lambda = \text{const}$ to $G \propto 1/k^2$, $\Lambda \propto k^2$ during a finite but, by assumption, small interval Δk_{tr} . The classical FRW solution is valid only for $t \lesssim t_{\text{tr}} - \Delta t_{\text{tr}}/2$, while the fixed point solution applies for $t \gtrsim t_{\text{tr}} + \Delta t_{\text{tr}}/2$. During the transition regime

$$t_{\text{tr}} - \Delta t_{\text{tr}}/2 \lesssim t \lesssim t_{\text{tr}} + \Delta t_{\text{tr}}/2 \quad (36)$$

the evolution is much more complicated, and we are not going to describe it explicitly. We assume that the system (3) applies also in the transition period, and that a more realistic version of the RG trajectory (30), (31) gives rise to a continuous and differentiable solution for all four functions. The interpolating solution is likely to exist because during the transition the cutoff identification may well be much more complicated than $k \propto 1/t$, the actual function $k = k(t, a(t), \dot{a}(t), \dots)$ being fixed to some extent by the requirement that (3) is consistent.

Thus our model provides an idealized description which ignores the transition regime, $\Delta t_{\text{tr}} \rightarrow 0$. This is a sensible approximation if Δt_{tr} is much smaller than t_{tr} . Since in reality the functions a, ρ, G and Λ do have a certain variation between $t_{\text{tr}} - \Delta t_{\text{tr}}/2$ and $t_{\text{tr}} + \Delta t_{\text{tr}}/2$, it is clear, then, that in the model these functions should be allowed to have some moderate discontinuity at $t = t_{\text{tr}}$. More precisely, we would consider it reasonable if $a(t \nearrow t_{\text{tr}})/a(t \searrow t_{\text{tr}})$, say, is a small number close to unity. On the other hand, if this ratio should turn out many orders of magnitude smaller than unity, say, then this means that the Universe undergoes an enormous ‘‘inflation’’ during the transition regime. In this case a crucial qualitative element would be missing from our description if we just consider the classical FRW solution and the fixed point solution explicitly. Hence the idealized model would not be very useful probably.

Let us now look at the properties of the extended IRFP model in detail. To start with, we assume that (32) and (33) hold true exactly so that $G(t)$ and $\Lambda(t)$ are continuous at the matching point. Eqs. (32) and (33) imply that

$$G_{<} \Lambda_{<} = g_* \lambda_* \quad (37)$$

This means that even if one allows for small discontinuities of G and Λ , the product $G_{<} \Lambda_{<}$ is of the order of 10^{-120} . As the cosmological constant problem in its original form (‘‘Why

is $\Lambda \ll m_{\text{Pl}}^2$?) is related to the smallness of this number, we see that the mechanism which has achieved this tiny value must have been operative already *before* the FRW era with $G_<$ and $\Lambda_<$ has started. (Later on we shall assume that the FRW era began before the time of nucleosynthesis.)

Using $t_{\text{tr}} = \xi/k_{\text{tr}}$ with ξ given by (17) we obtain for the time of the transition:

$$t_{\text{tr}}^2 = \frac{\xi^2}{k_{\text{tr}}^2} = \frac{8}{3(1+w)^2 \lambda_* k_{\text{tr}}^2} = \frac{8}{3(1+w)^2 \Lambda_<} \quad (38)$$

Hence, in terms of $\Lambda_<$ or $G_<$,

$$\begin{aligned} t_{\text{tr}} &= \frac{1}{(1+w)} \sqrt{\frac{8}{3\Lambda_<}} \\ &= \frac{1}{(1+w)} \sqrt{\frac{8G_<}{3g_*\lambda_*}} \end{aligned} \quad (39)$$

Another useful representation of t_{tr} in terms of the age of the Universe can be obtained by eliminating $g_*\lambda_*$ from the second line of (39) by virtue of (27) with $H_0 = 4/[3(1+w)t_0]$. The result is surprisingly simple:

$$t_{\text{tr}} = t_0 \sqrt{\frac{G_<}{G(t_0)}} \quad (40)$$

Now we are in a position to calculate $a(t_{\text{tr}})$ both from the fixed point solution $a(t) \equiv a_{\text{FP}}(t)$ of (15a) and the classical FRW solution $a(t) \equiv a_{\text{FRW}}(t)$ in (34). With (39) we obtain

$$a_{\text{FP}}(t_{\text{tr}}) = \left[\frac{\mathcal{M}G_<}{\Lambda_<} \right]^{1/(3+3w)} \quad (41)$$

and

$$a_{\text{FRW}}(t_{\text{tr}}) = C_w \left[\frac{\mathcal{M}G_<}{\Lambda_<} \right]^{1/(3+3w)} = C_w a_{\text{FP}}(t_{\text{tr}}) \quad (42)$$

where

$$C_w \equiv \left(\frac{\cosh(\sqrt{8}) - 1}{2} \right)^{1/(3+3w)} \quad (43)$$

In the following we continue the discussion for the most relevant equation of state $p = 0$, i.e. $w = 0$.

In this case the ratio of the two scale factors, C_w , has the numerical value $C_0 \approx 1.55$. It is encouraging to see that this number is indeed relatively close to unity. As $C_0 > 1$ the FRW scale factor at $t = t_{\text{tr}}$ is *larger* than the one of the fixed point regime. We discussed above

that, strictly speaking, the FRW solution $a_{\text{FRW}}(t)$ is valid only for $t \lesssim t_{\text{tr}} - \Delta t_{\text{tr}}/2$ and the fixed point solution $a_{\text{FP}}(t)$ applies only for $t \gtrsim t_{\text{tr}} + \Delta t_{\text{tr}}/2$. During the transition a more complicated solution interpolates smoothly between a_{FRW} and a_{FP} . The simplest possible behavior of the interpolating solution one could imagine is that $a(t)$ stays approximately constant between $t_{\text{tr}} - \Delta t_{\text{tr}}/2$ and $t_{\text{tr}} + \Delta t_{\text{tr}}/2$. If one then chooses Δt_{tr} such that

$$a_{\text{FRW}}(t_{\text{tr}} - \Delta t_{\text{tr}}/2) = a_{\text{FP}}(t_{\text{tr}} + \Delta t_{\text{tr}}/2) \quad (44)$$

the resulting scale factor is continuous and nondecreasing. Clearly, also a more complicated behavior of the exact solution is conceivable, but, even without knowing the details of the exact solution, the condition (44) gives us a first idea about the size of Δt_{tr} . Being interested in an approximate estimate only, it is actually more convenient to define Δt_{tr} in a slightly different way, by $a_{\text{FRW}}(t_{\text{tr}}) = a_{\text{FP}}(t_{\text{tr}} + \Delta t_{\text{tr}})$, which boils down to

$$C_0 = \frac{a_{\text{FP}}(t_{\text{tr}} + \Delta t_{\text{tr}})}{a_{\text{FP}}(t_{\text{tr}})} = \left(\frac{t_{\text{tr}} + \Delta t_{\text{tr}}}{t_{\text{tr}}} \right)^{4/3} \quad (45)$$

whence

$$\frac{\Delta t_{\text{tr}}}{t_{\text{tr}}} = C_0^{3/4} - 1 \approx 0.39 \quad (46)$$

Even though Δt_{tr} is not very much smaller than t_{tr} itself, the ratio (46) indicates that there can very well be a window in which the idealized model is useful for a first orientation.

Note that, as a consequence of the exact relation (16), the discontinuity of $\rho(t)$ is necessarily of the same order of magnitude as that of $a(t)$.

From now on we shall be slightly more specific and assume that the FRW era with $G = G_{<}$ and $\Lambda = \Lambda_{<}$ has started before the time of primordial nucleosynthesis already (with $w = 1/3$ then). This assumption allows us to fix the value of $G_{<}$. In fact, from the successful predictions of nucleosynthesis theory we know that the value of the cosmological Newton's constant during this epoch was very close to the laboratory value: $G(t_{\text{nucl}}) = G_{\text{exp}}$. Since, by assumption, $G(t_{\text{nucl}}) = G_{<}$, this entails

$$G_{<} = G_{\text{exp}} \quad (47)$$

With this identification, the transition time (40) reads

$$t_{\text{tr}} = t_0 \sqrt{\frac{G_{\text{exp}}}{G(t_0)}} \quad (48)$$

This equation is quite remarkable. It relates the time when the fixed point behavior started to the ratio of the laboratory value of Newton's constant and the cosmological Newton's constant. Using (23) we can reexpress this ratio in terms of Ω_M^{exp} :

$$t_{\text{tr}} = t_0 \sqrt{2 \Omega_M^{\text{exp}}(t_0)} \quad (49)$$

Eqs. (48) and (49) are our main results of this section.

It is convenient to characterize t_{tr} by the corresponding redshift z_{tr} . We have

$$1 + z_{\text{tr}} = \frac{a(t_0)}{a(t_{\text{tr}})} = \left(\frac{t_0}{t_{\text{tr}}} \right)^{4/3} \quad (50)$$

and

$$1 + z_{\text{tr}} = \left(\frac{G(t_0)}{G_{\text{exp}}} \right)^{2/3} = [2 \Omega_M^{\text{exp}}(t_0)]^{-2/3} \quad (51)$$

Which values of z_{tr} could we expect? The assumption $\Omega_M^{\text{exp}}(t_0) \gtrsim 1/100$ yields $t_{\text{tr}} \gtrsim t_0/7$ and $z_{\text{tr}} \lesssim 12$, for instance. A distinguished period during the “recent” evolution of the Universe is the era of galaxy formation at about $z \approx 3$, say. If we speculate that the fixed point behavior started during this era we have

$$z_{\text{tr}} \approx 3, \quad t_{\text{tr}} \approx \frac{t_0}{2.8} \quad (52)$$

This scenario corresponds to $\Omega_M^{\text{exp}}(t_0) \gtrsim 1/16$. It has been shown in ref. [19] that there are no growing “large” wavelength (which probably means super Hubble size) density perturbations in the fixed point regime. However, “small”-scale density perturbations can grow even in the fixed point regime. Hence $z_{\text{tr}} > 3$ is not necessarily excluded by the theory of structure formation.

We expect that if z_{tr} is too small and the transition happened only recently, the fixed point solution cannot provide an accurate description of the present Universe because the transient phenomena of the transition region are still visible to some extent. Let us write $\Delta t_{\text{FP}} \equiv t_0 - t_{\text{tr}}$ for the time which, according to the model, elapsed since the onset of the fixed point behavior. As a rough estimate we can say that the present Universe is already well within the fixed point regime, and the transient effects have become insignificant, provided $\Delta t_{\text{FP}} \gtrsim \Delta t_{\text{tr}}$. We rewrite this inequality as $\Delta t_{\text{FP}}/t_{\text{tr}} \gtrsim \Delta t_{\text{tr}}/t_{\text{tr}}$. Then its LHS is given by (50),

$$\frac{\Delta t_{\text{FP}}}{t_{\text{tr}}} = (1 + z_{\text{tr}})^{3/4} - 1, \quad (53)$$

and (46) yields $C_0^{3/4} - 1$ for the RHS. Hence we are already well within the fixed point regime if $1 + z_{\text{tr}} \gtrsim C_0$ or

$$z_{\text{tr}} \gtrsim 0.55 \tag{54}$$

Thus we have a wide range of z_{tr} -values where the model can be applied consistently.

The estimate (54) is of a rather intriguing order of magnitude. In fact, the most distant supernova analyzed in [22] and [23] has a redshift of about $z \approx 1$, while the highest redshift bin for the radio sources in [28] (see Section IV) is centered about $z = 3.6$. Thus, if the transition occurred relatively late, around $z = 0.5$, say, the current data might already tell us something about the transition from the FRW to the fixed point regime. This question will be discussed in detail in Sections III and IV.

D. Summary of the extended IRFP model

We investigated a simple cosmological model in which the IR fixed point regime of [16] is preceded by a classical FRW era with constant values of G and Λ . While the hypothesis of this FRW era does not introduce any unknown new parameter, it allows for a determination of the time when the Universe entered the fixed point regime. In a nutshell, this time, t_{tr} , obtains from the intersection point of the parabola $G_{\text{FP}} \propto t^2$ with the straight line $G_{\text{FRW}}(t) = G_{<}$. The transition time t_{tr} turns out to be given by the ratio of the cosmological and laboratory value of Newton's constant or, equivalently, by the matter energy density $\Omega_{\text{M}}^{\text{exp}}(t_0)$. If this density is of the order of the critical density, the ratio t_0/t_{tr} is close to unity, i.e. the transition happened only “recently”. In this sense the model solves the “coincidence problem”, the question why ρ and ρ_{Λ} happen to be of the same order of magnitude precisely today. In our model we have $\rho/\rho_{\Lambda} = 1$ at any time later than t_{tr} .

III. TYPE IA SUPERNOVAE AND THE IRFP COSMOLOGY

Recent supernova data from several sources (Supernova Cosmology Project [22], High Redshift Supernova Team [23]) provide a valuable tool in cosmological hypothesis testing, since they contain information about the luminosity distance function $d_L(z)$. In this section we shall apply the standard χ^2 test in order to analyze the viability of the IRFP hypothesis.

In the Appendix, an alternative approach based on median statistics [20, 21] and a Bayesian model selection criterion is discussed in detail.

A. The data set

The data set used in all of our analyses consists of the 18 low redshift type Ia SNe from the Calan-Tololo survey [26] plus 74 high redshift type Ia SNe, namely:

- 42 SNe discovered by the SCP, whose measured redshifts and apparent magnitudes are published in Perlmutter et al. [22];
- 32 SNe discovered by the HST, who reported their measured redshifts and distance moduli in Riess et al. [23].

This gives a total of 92 supernovae. The oldest, most distant supernova is SN 1997ck, with a redshift of $0.97 \equiv z_{\max}$.

B. Luminosity distance-redshift relations

Let us assume that, at time t_1 , a distant galaxy emits light which is detected on Earth at t_0 . The luminosity distance d_L to this galaxy is defined by the relation

$$\mathcal{F} = \frac{\mathcal{L}}{4\pi d_L^2} \quad (55)$$

where \mathcal{L} is the absolute luminosity of the source and \mathcal{F} is the measured flux. From the Robertson-Walker kinematics one obtains

$$d_L = \frac{a^2(t_0)}{a(t_1)} S \left(\int_{t_1}^{t_0} \frac{dt}{a(t)} \right) \quad (56)$$

where

$$S(x) = \begin{cases} \sin x & \text{for } K = +1 \\ x & \text{for } K = 0 \\ \sinh x & \text{for } K = -1 \end{cases} \quad (57)$$

Using $a(t_0)/a(t_1) = 1 + z$ we may rewrite the integral in (56) in terms of the redshift z :

$$\int_{t_1}^{t_0} dt \frac{a_0}{a(t)} = \int_0^z dz' \frac{1}{H(z')} \quad (58)$$

(The subscript “0” on any quantity denotes its value at $t = t_0$.) In particular for $K = 0$,

$$d_L(z) = \frac{1+z}{H_0} \int_0^z dz' \frac{H_0}{H(z')} \quad (59)$$

In order to calculate $H_0/H(z')$, a further distinction is necessary:

1. The *IRFP cosmology* has $K = 0$ and is given by (15) where we shall set $w = 0$ from now on. The corresponding luminosity distance as a function of the redshift of the source reads

$$d_L(z) = \frac{4(1+z)}{H_0} \left[(1+z)^{1/4} - 1 \right] \quad (60)$$

Eq. (60) is obtained either by inserting $a \propto t^{4/3}$ into (56) and eliminating t_1 in favor of z , or by using (59) with

$$H(z) = H_0 (1+z)^{3/4} \quad (61)$$

which follows from (19).

2. In standard *FRW cosmology* one has the familiar relationship

$$H(z) = H_0 \left[(1+z)^3 \Omega_{M0} + \Omega_{\Lambda 0} + (1+z)^2 \Omega_{K0} \right]^{1/2} \quad (62)$$

which can be used to derive

$$d_L(z) = \frac{(1+z)}{H_0 \sqrt{|\Omega_{K0}|}} S \left(\sqrt{|\Omega_{K0}|} \int_0^z dz' \left[(1+z')^3 \Omega_{M0} + \Omega_{\Lambda 0} + (1+z')^2 \Omega_{K0} \right]^{-1/2} \right) \quad (63)$$

As for the actual form of the function S , eq. (10) shows that the cases $K = +1, 0$ and -1 are realized if $\Omega_{K0} < 0$, $\Omega_{K0} = 0$ and $\Omega_{K0} > 0$, respectively.

3. In the *extended IRFP model* introduced in subsection II C we combine a $K = 0$ FRW cosmology, valid for $t < t_{\text{tr}}$ ($z > z_{\text{tr}}$), with the fixed point cosmology which applies for $t > t_{\text{tr}}$ ($z < z_{\text{tr}}$). For arguments $z < z_{\text{tr}}$, the corresponding function $d_L(z)$ is given by (60). For arguments $z > z_{\text{tr}}$ we divide the z' -integral of (59) in a IRFP plus a FRW piece:

$$d_L(z) = \frac{1+z}{H_0} \left\{ \int_0^{z_{\text{tr}}} dz' \left[\frac{H_0}{H(z')} \right]_{\text{IRFP}} + \int_{z_{\text{tr}}}^z dz' \left[\frac{H_0}{H(z')} \right]_{\text{FRW}} \right\} \quad (64)$$

The integrand of the IRFP piece is given by (61) and for the FRW term we use (62) with $\Omega_{K0} = 0$:

$$d_L(z) = \frac{1+z}{H_0} \left\{ \int_0^{z_{\text{tr}}} dz' (1+z')^{-3/4} + \int_{z_{\text{tr}}}^z dz' \left[(1+z')^3 \tilde{\Omega}_{M0} + \tilde{\Omega}_{\Lambda 0} \right]^{-1/2} \right\} \quad (65)$$

The quantities $\tilde{\Omega}_{M0}$ and $\tilde{\Omega}_{\Lambda0} = 1 - \tilde{\Omega}_{M0}$ are not the physical densities at $t = t_0$, these are $\Omega_{M0} = \Omega_{\Lambda0} = 1/2$, but rather fictitious values which would result from using the standard FRW differential equations also for t between t_{tr} and t_0 . The quantities $\tilde{\Omega}_{M0}$ and $\tilde{\Omega}_{\Lambda0}$ are determined by the requirement that the FRW- and the IRFP-solution match at $z = z_{\text{tr}}$; they depend on z_{tr} therefore.

In the present context it is most convenient to define t_{tr} by the requirement that $\Omega_M(t)$ and $\Omega_\Lambda(t)$ are continuous at the transition.³ Then the specific FRW theory which connects to the fixed point cosmology is singled out by the requirement

$$\Omega_\Lambda^{\text{FRW}}(t_{\text{tr}}) = \Omega_\Lambda^{\text{IRFP}}(t_{\text{tr}}) = 1/2 \quad (66)$$

and similarly for Ω_M . On the FRW side we can use the general result⁴

$$\Omega_\Lambda(z) = \Omega_{\Lambda0} \left[(1+z)^3 \Omega_{M0} + \Omega_{\Lambda0} + (1+z)^2 \Omega_{K0} \right]^{-1} \quad (67)$$

in order to relate $\Omega_\Lambda^{\text{FRW}}(t_{\text{tr}})$ to $\tilde{\Omega}_{\Lambda0}$. Letting $z = z_{\text{tr}}$, $\Omega_\Lambda(z_{\text{tr}}) = 1/2$, $\Omega_{\Lambda0} \rightarrow \tilde{\Omega}_{\Lambda0}$, $\Omega_{M0} \rightarrow \tilde{\Omega}_{M0}$, eq. (67) yields

$$\tilde{\Omega}_{\Lambda0} = (1 + z_{\text{tr}})^3 \tilde{\Omega}_{M0} \quad (68)$$

which, with $\tilde{\Omega}_{M0} = 1 - \tilde{\Omega}_{\Lambda0}$, leads to

$$\tilde{\Omega}_{M0} = \frac{1}{1 + (1 + z_{\text{tr}})^3} \quad (69)$$

$$\tilde{\Omega}_{\Lambda0} = \frac{(1 + z_{\text{tr}})^3}{1 + (1 + z_{\text{tr}})^3} \quad (70)$$

Using (69) and (70) in (65) we obtain the final result for the luminosity distance in the case $z > z_{\text{tr}}$:

$$d_L(z) = \frac{1+z}{H_0} \left\{ 4(1+z_{\text{tr}})^{1/4} - 4 + \left[1 + (1+z_{\text{tr}})^3 \right]^{1/2} \int_{z_{\text{tr}}}^z dz' \left[(1+z')^3 + (1+z_{\text{tr}})^3 \right]^{-1/2} \right\} \quad (71)$$

It is customary to express luminosity distances in terms of the distance modulus $\mu_0 \equiv m(z) - M$ according to

$$m(z) = M + 5 \log_{10} \left(\frac{d_L(z)}{1 \text{ Mpc}} \right) + 25 \quad (72)$$

³ The t_{tr} thus defined coincides with the one from subsection II C within Δt_{tr} .

⁴ Eq. (67) follows from (62) by noting that $\rho_\Lambda = \text{const}$ in the standard case, and that $\rho_{\text{crit}} \propto H^2$.

where m and M are the apparent and absolute magnitude, respectively. Measuring d_L in units of the present Hubble radius, $1/H_0$, the dependence of the apparent magnitude on the “Hubble-free” luminosity distance $H_0 d_L$ reads

$$m(z) = \mathcal{M} + 5 \log_{10} \left(H_0 d_L(z) \right) \quad (73)$$

where⁵

$$\mathcal{M} \equiv M - 5 \log_{10} (H_0 \cdot 1 \text{ Mpc}) + 25 \quad (74)$$

is constant within an ensemble of standard candles.

The HzST results are presented in terms of the distance modulus, while the SCP published the estimated effective B -band magnitude m_B^{eff} which relates to the HzST results through

$$m_B^{\text{eff}} = M_B + \mu_0 \quad (75)$$

where M_B is the peak B -band absolute magnitude of a standard type Ia supernova. We chose to translate the HzST data from distance moduli into apparent magnitudes, leaving the SCP data unchanged.

In the expression for the apparent magnitude, M_B and H_0 appear only in the combination $\mathcal{M}_B = M_B - 5 \log_{10}(H_0 \cdot 1\text{Mpc}) + 25$. We have used the value of \mathcal{M}_B that is obtained from the analysis of the low-redshift SN sample of the Calan-Tololo survey [26] alone. If $z \ll 1$, the expression (73) for the apparent magnitude becomes

$$m_B(z) = \mathcal{M}_B + 5 \log_{10} z \quad (76)$$

Fitting the measured apparent magnitudes to this formula yields $\mathcal{M}_B = -3.32$.

The total data set now consists of 92 measured apparent magnitudes m_B^{meas} , henceforth denoted m_i^{meas} , $i = 1, \dots, 92$, which must be compared to the theoretical expectation for the Hubble-free expression for the apparent magnitude,

$$m_B(z) = \mathcal{M}_B + 5 \log_{10} \left(H_0 d_L(z) \right) \quad (77)$$

Fig. 1 displays the apparent magnitudes m_i^{meas} as a function of the corresponding measured redshifts z_i . The error bars on the data points indicate the statistical errors σ_i of

⁵ There should arise no confusion with the invariant (16) with the same name \mathcal{M} which is also customary.

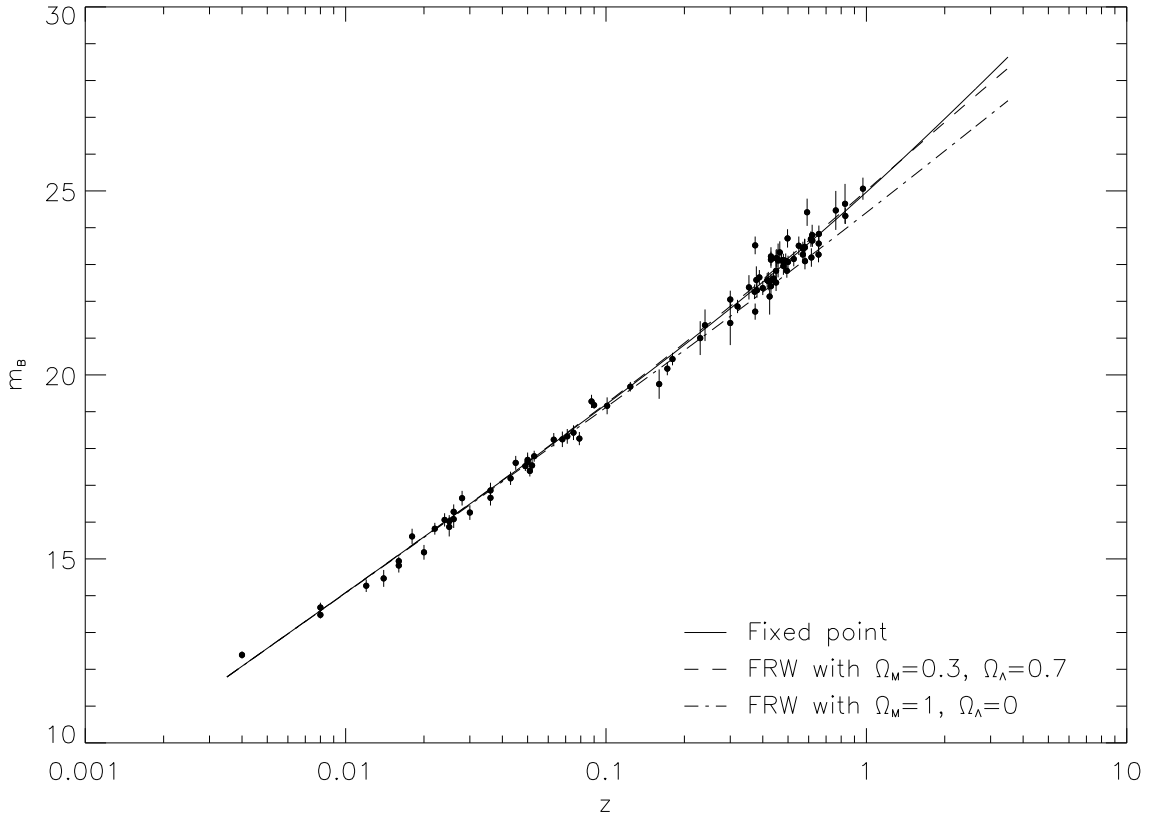


FIG. 1: The measured apparent magnitudes of the supernovae as a function of their redshift. The continuous line represents the prediction of the IRFP cosmology, the dashed one is the best-fit FRW model, and the dot-dashed line is a flat FRW model with zero cosmological constant.

m_i^{meas} estimated by SCP and HzST, respectively. Fig. 1 also shows the theoretical curve (77) with the function $d_L(z)$ pertaining to three different cosmological models: the IRFP model (without a FRW part), a FRW model with $\Omega_{M0} = 0.3$, $\Omega_{\Lambda0} = 0.7$, and a FRW model with $\Omega_{M0} = 1$, $\Omega_{\Lambda0} = 0$. The second model is the one which, in the framework of standard FRW cosmologies, fits the data best. The question is whether the IRFP leads to an even better fit.

C. χ^2 analysis of the currently available data

The standard χ^2 test is the most common choice in order to quantify the agreement between the predictions of some cosmological model and the supernova data. From the

triples $(z_i, m_i^{\text{meas}}, \sigma_i)$, $i = 1, \dots, 92$, provided by the dataset described in III A we have to compute

$$\chi^2 = \sum_{i=1}^{92} \left[\frac{m_i^{\text{meas}} - m_i^{\text{theor}}}{\sigma_i} \right]^2 \quad (78)$$

where $m_i^{\text{theor}} \equiv m_B(z_i)$ is the theoretical value predicted by eq. (77) with the function $d_L(z)$ computed within a specific model. As for the fixed point model, we must distinguish the cases $z_{\text{tr}} > z_{\text{max}}$ and $z_{\text{tr}} < z_{\text{max}}$. In the former, the Universe had already entered the fixed point regime by the time the oldest supernova exploded; in the latter, some of the supernova events took place during the preceding FRW era, and their photons detected by our telescopes have witnessed the transition to the fixed point regime.

If $z_{\text{tr}} > z_{\text{max}}$ then $d_L(z_i)$ is given by (60) for all supernovae. The evaluation of the sum (78) yields a value of χ^2 per degree of freedom (χ^2/dof) of 1.59. In Table I we compare this number to the corresponding χ^2 values for three competing FRW cosmologies:

- The best-fit FRW model with vanishing cosmological constant and Ω_{M0} anywhere in the interval $[0, 3]$;
- The best-fit FRW model with $\Omega_{M0} \in [0, 3]$ and $\Omega_{\Lambda0} \in [-1, 3]$ such that $\Omega_{M0} + \Omega_{\Lambda0} = 1$, i.e. spacetime is spatially flat;
- The best-fit FRW model with $\Omega_{M0} \in [0, 3]$ and $\Omega_{\Lambda0} \in [-1, 3]$ arbitrary.

We see that the χ^2/dof value of the IRFP cosmology is about the same as those for the FRW models. Taking the numbers in Table I at face value, the fixed point model performs even slightly better than its FRW competitors. This is a very encouraging result, in particular since, contrary to the FRW models, *the fixed point model has no free parameters* which could be adjusted.

Up to here we assumed that $z_{\text{tr}} > z_{\text{max}}$ so that even the oldest supernova in the dataset would not "know" about the onset of the fixed point epoch. Assuming the opposite case $z_{\text{tr}} < z_{\text{max}}$ now, some of the older supernovae exploded already during the FRW era which, according to the extended IRFP model, preceded the fixed point epoch. The function $d_L(z)$ of the extended IRFP model depends parametrically on z_{tr} . For supernovae with $z_i < z_{\text{tr}}$ the value of $d_L(z_i)$ is given by equation (60), while for $z_i > z_{\text{tr}}$ eq. (71) must be used. As

a consequence, χ^2 is a function of z_{tr} now, and in principle one could hope to extract the value of z_{tr} from the data by looking where $\chi^2 = \chi^2(z_{\text{tr}})$ is minimum. In the ideal case the function $\chi^2(z_{\text{tr}})$ would have a pronounced minimum at some value of z_{tr} , and we would then be entitled to conclude that the fixed point regime started at this redshift most probably.

Using again the data set of subsection III A we obtain the function $\chi^2 = \chi^2(z_{\text{tr}})$ which is plotted in Fig. 2. Obviously there is no strongly preferred value of z_{tr} . There seems to be a minimum at $z_{\text{tr}} \approx 0.18$, but it is too shallow to derive any statistically significant conclusion from it.

Thus we must conclude that the statistical quality of the currently available supernova data is not good enough in order to discriminate between the fixed point model proper (without a FRW era) and the one-parameter family, parametrized by z_{tr} , of extended fixed point models.

D. χ^2 analysis of Monte Carlo data for SNAP

It is an important question whether it would be possible to detect a "smoking gun" of the transition to the IRFP regime in the supernova data if a better statistics were available. In fact, the *SNAP* (*Supernova Acceleration Probe*) satellite is aimed to improve this statistics

TABLE I: The value of χ^2 per degree of freedom for several cosmological models (the errors on the best-fit parameter values correspond to the $1\text{-}\sigma$ confidence region).

Model ^a	χ^2/dof	Parameter values at minimum
Fixed point model ($z_{\text{tr}} > z_{\text{max}}$)	1.59	-
Extended fixed point model	1.60	$z_{\text{tr}} = 0.17_{-0.10}^{+0.80}$
Best-fit FRW with $\Omega_{\Lambda 0} = 0$	1.62	$\Omega_{M0} = 0.00^{+0.05}$
Best-fit FRW with $\Omega_{\Lambda 0} + \Omega_{M0} = 1$	1.60	$\Omega_{M0} = 0.40_{-0.05}^{+0.10}$
Best-fit FRW	1.62	$\Omega_{M0} = 0.25_{-0.25}^{+0.65}, \Omega_{\Lambda 0} = 0.40_{-0.40}^{+0.75}$

^aThe variation intervals for Ω_{M0} and $\Omega_{\Lambda 0}$ in the fits are $[0,3]$ and $[-1,3]$, respectively. The transition redshift z_{tr} goes from 0 to 0.97, the redshift of the farthest SN in the set.

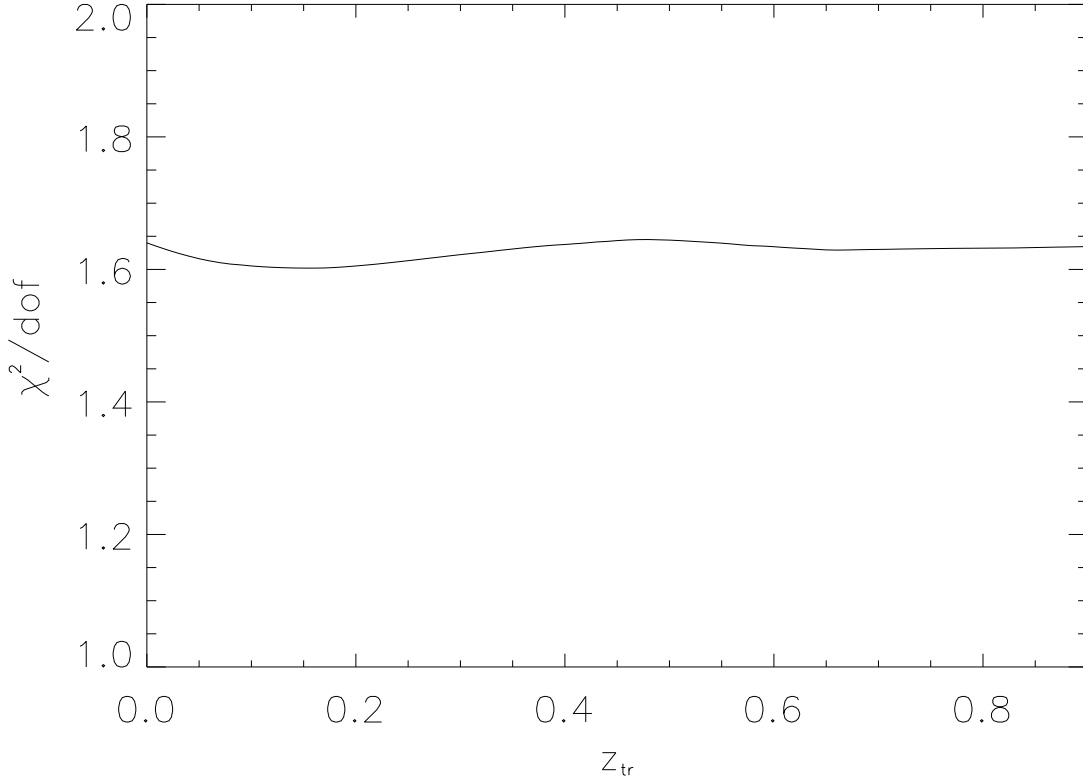


FIG. 2: The χ^2 value of the extended IRFP model as a function of the redshift z_{tr} obtained from the currently available data set.

at a significant level. Its goal is to obtain a super data set more than one order of magnitude larger than the currently available one, with an improved control over systematic errors, to redshifts up to about $z \approx 1.7$. We therefore decided to simulate the expected results in order to forecast the impact of this enlarged data set on the constraints for z_{tr} . In particular we used the SNOC code, developed by A.Goobar *et al.* [27], which takes into account gravitational interactions (lensing) and extinction by dust, both in the host galaxy and along the line-of-sight, and modified it by implementing our new distance-redshift formula.

The modified SNOC code based upon the extended IRFP model was used to generate 4 different Monte Carlo data sets, each consisting of 2000 type Ia supernovae in the redshift interval $[0.1, 1.8]$. The 4 simulations differed with respect to the transition redshift $z_{\text{tr}}^{\text{simul}}$ of the underlying IRFP model; we chose $z_{\text{tr}}^{\text{simul}} = 0.2, 0.4, 0.6$ and 1.0 , respectively. We then performed a χ^2 -analysis of the 4 data sets as we did with the "real" data in the previous

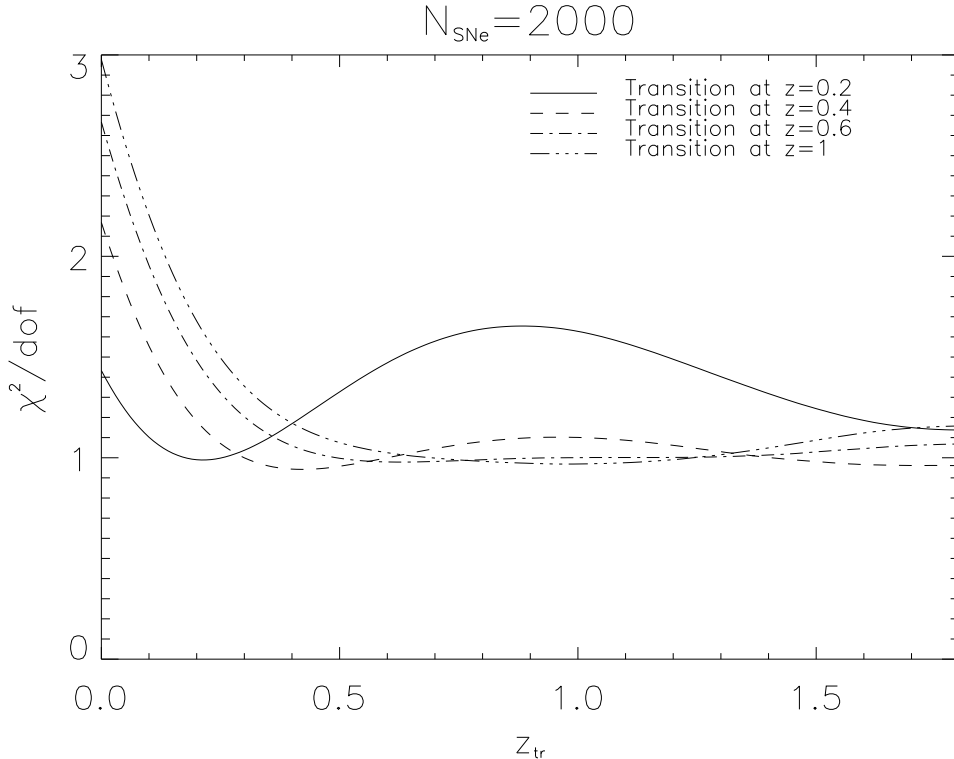


FIG. 3: The function $\chi^2(z_{\text{tr}})$ from a simulated data set of 2000 supernovae for various values of the transition redshift $z_{\text{tr}}^{\text{simul}}$.

subsection. Fig. 3 shows the resulting χ^2 as a function of z_{tr} (not to be confused with $z_{\text{tr}}^{\text{simul}}$). We find that, if the transition took place late enough, at a redshift of 0.2, say, there is a clear minimum in the $\chi^2(z_{\text{tr}})$ curve, and it should be possible to determine z_{tr} from the SNAP data⁶. On the other hand, if it occurred much earlier, at a redshift of 1.0, say, the $\chi^2(z_{\text{tr}})$ curve does not prefer any specific value of z_{tr} . For $z_{\text{tr}} \gtrsim 0.5$ this curve is almost flat. This is related to the fact that, if $z_{\text{tr}} \gtrsim 1$, the luminosity distance functions $d_L(z)$ of (60) and (71) are virtually identical for arguments $z \in [0, 2]$, say.

The lesson we learn from this Monte Carlo investigation is that, if we improve the statistics by a factor of about 10, there is a significant hope of either actually detecting the transition to the fixed point regime if $z_{\text{tr}} \lesssim 0.5$, or at least of putting a lower bound on z_{tr} if $z_{\text{tr}} \gtrsim 0.5$.

In the Appendix and in Section V we resume the analysis of the currently available

⁶ In view of the discussion which led to the estimate (54) it is clear, however, that a quantitatively correct description of this late transition would require a more sophisticated model than that of Section II.

“real” supernova data. Since they are anyhow not sufficient to determine z_{tr} we assume that $z_{\text{tr}} > z_{\text{max}}$ there.

IV. COMPACT RADIO SOURCES AND THE IRFP COSMOLOGY

In the previous section we have shown how a class of astronomical objects of well-known intrinsic properties can help probing the cosmic evolution via the luminosity distance-redshift relation.

A similar, yet independent test is based on the angular diameter distance-redshift relation. The *angular diameter distance* $d_A(z)$ of an object with redshift z and proper diameter l which subtends an angle θ as seen by a terrestrial observer is defined as

$$d_A(z) \equiv \frac{l}{\theta} = \frac{D/H_0}{\theta} \quad (79)$$

where we have introduced the characteristic angular size $D \equiv lH_0$ which is to be interpreted as an angle given in milliarcseconds (mas). By measuring the object’s redshift and θ -angle one can compute its value of $d_A(z)$ and compare it to some particular cosmological model, provided its diameter l is known. By comparing the predictions of several different models, the one which best fits the data can then be established. Of course, a class of *standard rods* (objects with the same characteristic extension l) is needed in order for this determination of $d_A(z)$ to be viable. Recently [28], with some manipulation and redshift-binning, a set of 330 compact radio sources has been applied to this purpose, thus giving the opportunity to constrain the free parameters of several cosmologies, from FRW and power-law models to cardassian expansion scenarios [28, 29, 30].

This section intends to address precisely the issue of confronting the IRFP model with the new data. The statistical framework is analogous to the one adopted in III: both the proper and extended versions of the IRFP model are compared to FRW cosmologies via the χ^2 test. The χ^2 test for the extended IRFP model is applied to the data set in order to give an estimate of the transition time t_{tr} .

A. The data set

The class of standard objects to be used as distance indicators is compact ($\lesssim 100$ pc) radio sources. Specifically, the set consists of 330 sources with redshifts z_i in the interval

[0.011, 4.72] and angular diameters θ_i , extracted from 5 GHz VLBI contour maps in the literature, as reported by Gurvits et al. [28].

Several reasons point out why these are likely to be standard objects: first, evolutionary effects are expected to be negligible with respect to galaxies or extended two-lobes radio sources, since the characteristic time scale of the former (some ten years) is very tiny compared to the age of the universe, or to the Hubble time H_0^{-1} . Second, while the physics of extended systems is more likely to be influenced by the different properties of the intergalactic medium encountered at different redshifts, the features of compact sources can in principle be described by a few parameters, like the mass of the central black hole, the magnitude of the magnetic field and of the angular momentum, and a few more.

Three tasks have thus to be completed before the data set can be applied to the cosmological analyses:

- (i) To control and put limits on the few basic parameters governing the radio source, so as to have a collection of objects which is as uniform as possible;
- (ii) To homogenize the set, which has been assembled from contour maps published by different collaborations, rather than from a unique set of observations;
- (iii) To investigate possible evolutionary effects (linear size - redshift dependence), as well as linear size - luminosity and linear size - spectral index dependences, and minimize their influence on the cosmological implications.

To these aims, Gurvits et al. [28] restrict the set by retaining only those sources with luminosity $Lh^2 \geq 10^{26}$ W/Hz and spectral index $-0.38 \leq \alpha \leq 0.18$. Since a moderate dependence of α on the angular size seems to be established (see Fig. 7 in [28]), the last relation has the further effect of constraining the dimensions of the sources.

The new group of 145 sources is then binned into 12 redshift intervals, and a median redshift and angular size is calculated for each one, together with the standard deviation σ_i . This procedure has the additional effect of reducing the influence of particularly large objects in the set, and providing simple means to deal with unresolved sources (see cases J, L and S in [28] for details).

The final data set consists of 12 triples $(z_i, \theta_i, \sigma_i)$ in the redshift interval [0.52, 3.6]. The data points, together with the three curves representing the proper IRFP prediction and the

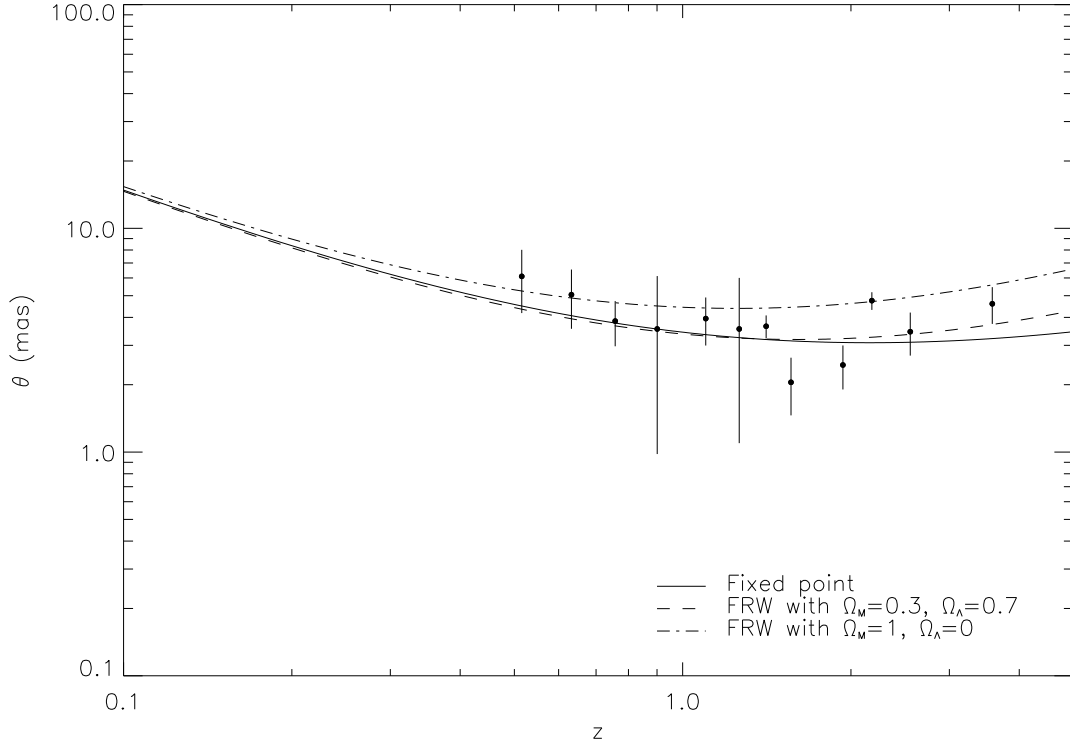


FIG. 4: The 12 data points (with corresponding uncertainties) and the theoretical predictions of the proper IRFP model and of the FRW models with $\Omega_M = 0.3, \Omega_\Lambda = 0.7$ and with $\Omega_M = 1, \Omega_\Lambda = 0$. The angular size D is assumed to equal its best-fit value $D = 1.30$.

FRW models with $\Omega_M = 0.3, \Omega_\Lambda = 0.7$ and with $\Omega_M = 1, \Omega_\Lambda = 0$, are presented in Fig. 4.

B. The angular diameter distance-redshift relation

From (79), following simple reasoning, one can easily show that in any spatially flat FRW spacetime

$$d_A(z) = \frac{d_L(z)}{(1+z)^2} = \frac{1}{H_0(1+z)} \int_0^z dz' \frac{H_0}{H(z')} \quad (80)$$

In III B we demonstrated that, in the extended IRFP model, for z greater than z_{tr} ,

$$\int_0^z dz' \frac{H_0}{H(z')} = 4(1+z_{\text{tr}})^{1/4} - 4 + \left[1 + (1+z_{\text{tr}})^3\right]^{1/2} \int_{z_{\text{tr}}}^z dz' \left[(1+z')^3 + (1+z_{\text{tr}})^3\right]^{-1/2} \quad (81)$$

while, for $z < z_{\text{tr}}$,

$$\int_0^z dz' \frac{H_0}{H(z')} = 4 \left[(1+z)^{1/4} - 1 \right] \quad (82)$$

It is evident from the above formulas that $d_A(z)$ also depends on the transition time, as long as the transition does not occur at a redshift z_{tr} which is greater than the maximum z of the sources in the data set ($z_{\text{max}} \approx 3.6$, see below.). We can therefore investigate the possibility of a transition to the fixed point regime in the redshift interval $[0, 3.6]$. This window is much larger than the one allowed by the supernova set adopted in III.

C. χ^2 analysis and determination of the transition time

A χ^2 function can thus be constructed in the usual manner:

$$\chi^2(z_{\text{tr}}, D) = \sum_{i=1}^{12} \left[\frac{\theta(z_i; z_{\text{tr}}) - \theta_i}{\sigma_i} \right]^2 \quad (83)$$

Here θ_i stands for the observed values of the angular size with errors σ_i , and

$$\theta(z_i; z_{\text{tr}}) = \frac{l}{d_A(z_i)} = \frac{D}{H_0 d_A(z_i)}$$

is the theoretical value. Let us note that the χ^2 value is also a function of the ‘‘Hubble free’’ diameter D of the source (it does not depend on H_0 though; see Eq.(80) for $d_A(z)$). The neatest way to solve this problem is to calculate a 2-dimensional χ^2 in the parameter space of z_{tr} and D , and then marginalize over D to make the results independent of its value [29]. The level contours for the probability $P(z_{\text{tr}}, D)$, associated to $\chi^2(z_{\text{tr}}, D)$ are shown in Fig. 5. $P(z_{\text{tr}}, D)$ is maximum at ($z_{\text{tr}} = 0.08, D = 1.3$ mas), where χ^2 has a corresponding value of 1.86. In Table II, this result is compared to other cosmologies. Marginalizing over D , i.e. defining a new probability as

$$\tilde{P}(z_{\text{tr}}) = \frac{\int_0^2 dD P(z_{\text{tr}}, D)}{\max [P(z_{\text{tr}}, D)]} \quad (84)$$

one obtains the probability distribution for z_{tr} alone, as shown in Fig. 6.

Clearly, the situation is even more problematic than for SNe Ia: the probability $\tilde{P}(z_{\text{tr}})$ hardly seems to vary, and a determination of z_{tr} is by no means possible with the current data. However, again we may conclude that the IRFP model proper performs as well as standard cosmology.

V. BEYOND THE IRFP MODEL: GENERAL POWER LAW SOLUTIONS

In this section we are going to put the fixed point cosmology into a more general perspective by “embedding” it into a broader class of cosmologies with a time dependent G and Λ . Let us give up for a moment the idea that the t -dependence of $G(t)$ and $\Lambda(t)$ stems from an underlying RG trajectory via some identification $k \equiv k(t)$. Then we are left with the system of equations (3a,3b,3c) without (3d). This system has been studied in the literature already long ago [31]. The problem is that (3a,3b,3c) is underdetermined, so that in order to obtain a unique solution one has to “invent” some additional condition on a, ρ, G and Λ on an *ad hoc* basis. For instance, without providing a deeper explanation, it was assumed [31] that Newton’s constant follows a power law $G(t) \propto t^n$ with an arbitrary, not necessarily integer exponent n . With this additional equation, the system (3a,3b,3c) has the following

TABLE II: The value of χ^2 per degree of freedom for several cosmological models (the errors on the best-fit parameter values correspond to the 1- σ confidence region).

Model ^a	χ^2/dof	Parameter values at minimum
Fixed point model ($z_{\text{tr}} > z_{\text{max}}$)	1.88	$D = 1.47^{+0.06}_{-0.07}$
Extended fixed point model	1.86	$z_{\text{tr}} = 0.08^{+0.80}_{-0.08}, D = 1.30^{+0.30}_{-0.13}$
Best-fit FRW with $\Omega_{\Lambda 0} = 0$	1.91	$\Omega_{M0} = 0.55^{+0.20}_{0.20}, D = 1.20^{+0.30}_{-0.30}$
Best-fit FRW with $\Omega_{\Lambda 0} + \Omega_{M0} = 1$	1.86	$\Omega_{M0} = 0.60^{+0.15}_{-0.15}, D = 1.20^{+0.30}_{-0.30}$
Best-fit FRW	1.91	$\Omega_{M0} = 0.15^{+1.65}_{-0.05}, \Omega_{\Lambda} = 1.20^{+0.15}_{-2.20}, D = 1.80^{+0.30}_{-0.90}$

^aThe variation intervals for Ω_{M0} and $\Omega_{\Lambda 0}$ in the fits are [0,3] and [-1,3], respectively. The transition redshift z_{tr} goes from 0 to 4.

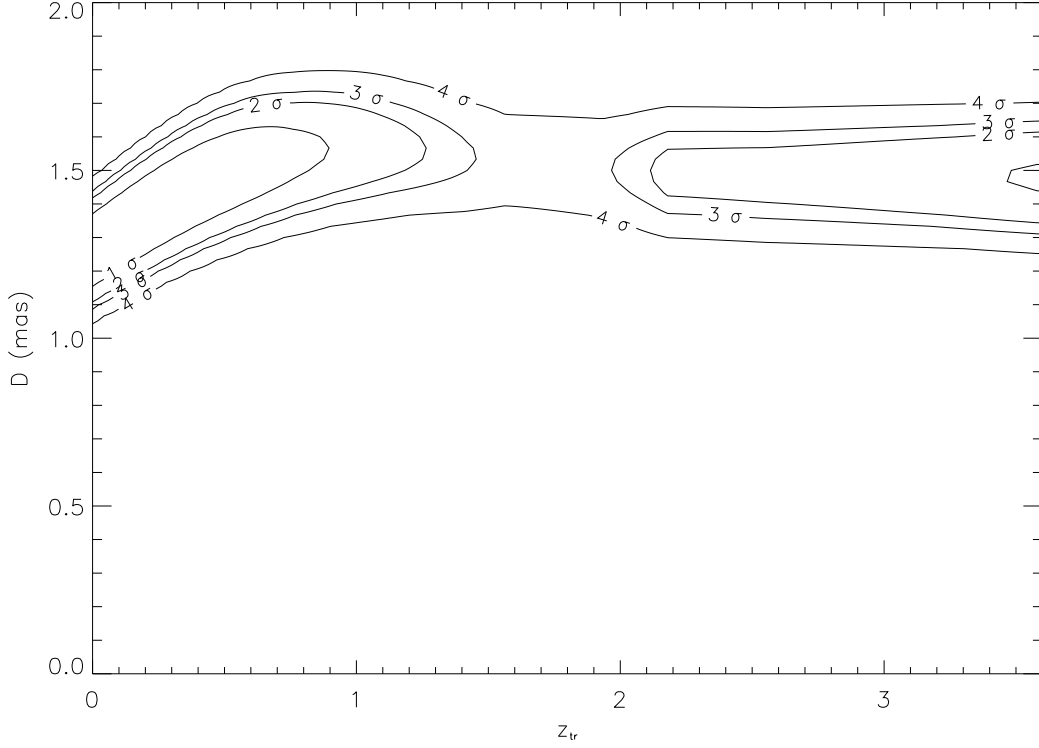


FIG. 5: Contour levels for the probability $P(z_{\text{tr}}, D)$.

solution for $K = 0$:

$$a(t) = \left[\frac{3(1+w)^2}{2(n+2)} \mathcal{M} C \right]^{1/(3+3w)} t^{(n+2)/(3+3w)} \quad (85a)$$

$$\rho(t) = \frac{(n+2)}{12\pi (1+w)^2 C} \frac{1}{t^{n+2}} \quad (85b)$$

$$G(t) = C t^n \quad (85c)$$

$$\Lambda(t) = \frac{n(n+2)}{3(1+w)^2} \frac{1}{t^2} \quad (85d)$$

Actually (85) describes a 2-parameter family of solutions labeled by the parameters \mathcal{M} and C . The fixed point cosmology (15) is the special case of (85) which is obtained by setting $n = 2$ and $C = 3(1+w)^2 g_* \lambda_*/8$. In fact, the exponent $n = 2$ is an unambiguous prediction of the fixed point hypothesis. It obtains not only for the simple cutoff identification $k \propto 1/t$ but even for an arbitrary function $k = k(t)$. This can be seen as follows. On the one hand we have, in the fixed point regime, $G(t)\Lambda(t) = G(k)\Lambda(k) = g_* \lambda_*$; on the other hand, eqs. (85c) and (85d) yield $G(t)\Lambda(t) = \text{const} \neq 0$ if, and only if, $n = 2$.

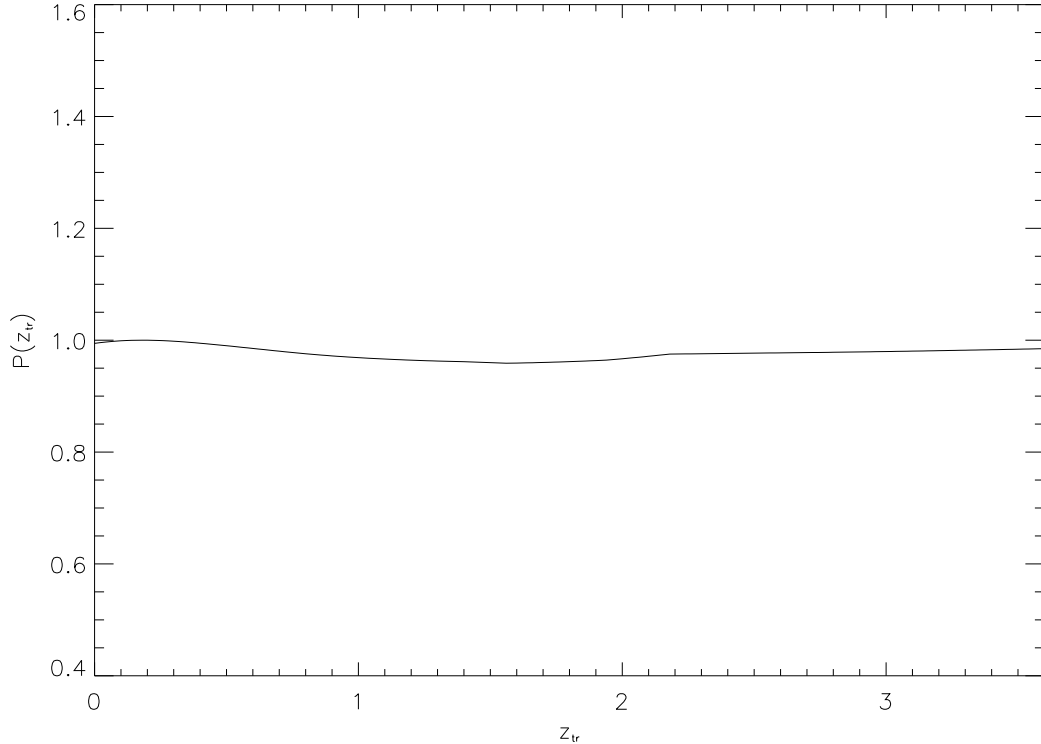


FIG. 6: The marginalized probability $\tilde{P}(z_{\text{tr}})$. A shallow maximum can be seen at $z_{\text{tr}} = 0.16$.

The luminosity distance for the models (85) is easily worked out. It is independent of \mathcal{M} and C , but it does depend on the exponent n . For a power law expansion $a(t) \propto t^\alpha$ we have in general

$$d_L(z) = \left(\frac{\alpha}{\alpha - 1} \right) \frac{(1+z)}{H_0} [(1+z)^{1-1/\alpha} - 1] \quad (86)$$

and (85a) yields in particular

$$\alpha = \frac{n+2}{3+3w} \quad (87)$$

We used the currently available supernova data in order to test the cosmologies (85). Proceeding as in Section III C, we performed a χ^2 analysis where m_i^{theor} was computed from the luminosity distance (86), (87) with $w = 0$, i.e. for $\alpha = (n+2)/3$. Fig. 7 displays the resulting χ^2 values as a function of the exponent n . Quite remarkably, we observe a clear minimum of χ^2 at $n = 2$, which is precisely the exponent predicted by the fixed point model. Stated differently, in the space of all cosmological models with a power law expansion $a \propto t^\alpha$ it seems to be exactly the $t^{4/3}$ -expansion of the IRFP model which fits the supernova data best.

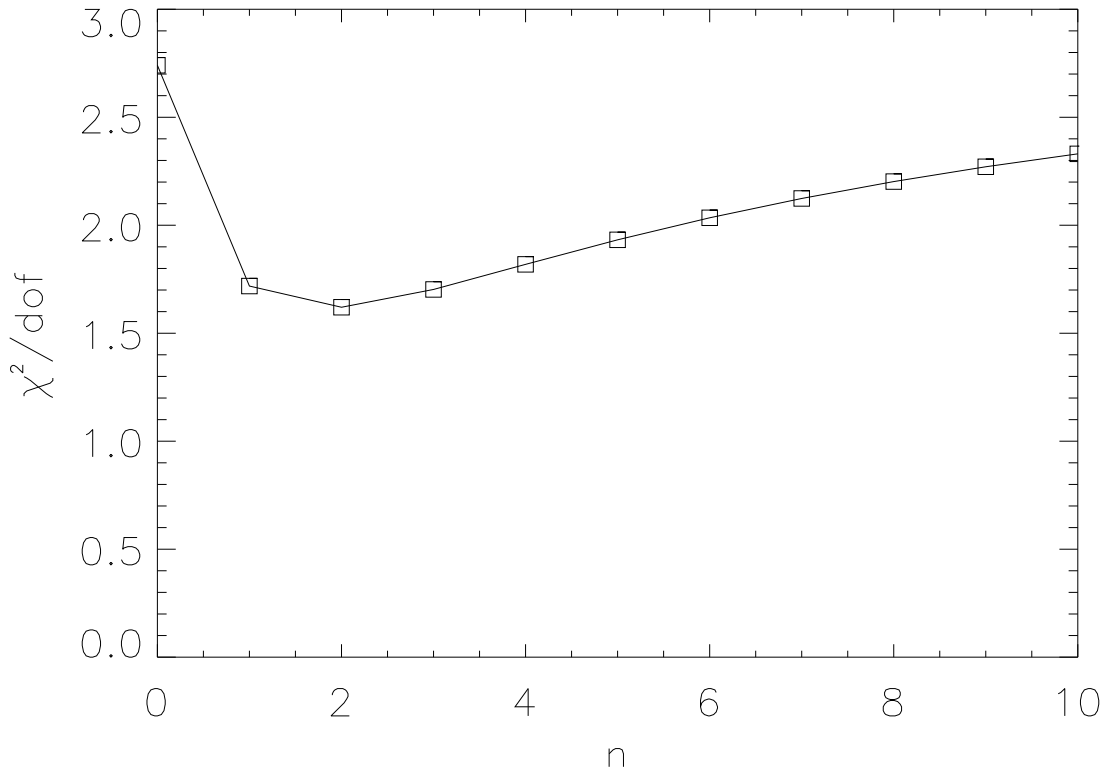


FIG. 7: The χ^2 values of the general power law models as a function of the exponent n .

VI. CONSTRAINTS ON z_{tr} FROM THE CMBR FIRST ACOUSTIC PEAK

The recent data from WMAP have determined the position of the first acoustic peak in the CMBR spectrum with great accuracy [32]. The spectrum depends on the complicated interplay between spacetime geometry and microphysics of the recombination era but the position of the first Doppler peak is essentially a measure of the angular size of the sound horizon, $\Delta\theta_s$, at the recombination epoch ($z_{\text{rec}} \approx 1300$). One has

$$\ell_1 \propto \frac{1}{\Delta\theta_s} \Big|_{z=z_{\text{rec}}} = \frac{d_A(z_{\text{rec}})}{d_H^S(z_{\text{rec}})} \quad (88)$$

where $d_A(z_{\text{rec}})$ is the angular diameter distance to the surface of last scattering, and $d_H^S(z_{\text{rec}})$ is the proper radius of the sound horizon at decoupling [33]. The precise proportionality factor on the LHS of (88) is determined by the microscopic model of the recombination. In standard FRW cosmology $\Delta\theta_s$ ranges from $\approx 0.85^\circ$ for a simple $\Lambda = 0$ model, to about $\approx 0.60^\circ$, in a more refined calculation [34]. Thus, strictly speaking the $\Delta\theta_s$ -value inferred

from a given measured multipole number ℓ_1 is model dependent, but the model dependence changes $\Delta\theta_s$ at most by a factor of order unity. Taking it for granted that $\Delta\theta_s$ is about one degree or slightly less, i.e. of the order of magnitude predicted by standard cosmology, we can derive an upper bound on z_{tr} in the following way.

The key observation is that both $d_A(z_{\text{rec}})$ and $d_H^S(z_{\text{rec}})$ tend to *increase* when we replace a piece of FRW evolution by the FP evolution. For z_{tr} small enough, their ratio $\Delta\theta_s$ stays almost constant.

As for $d_A(z_{\text{rec}})$, Eq.(80) with (86) provides us with $d_A(z)$ for a power law expansion $a(t) \propto t^\alpha$. We can use this formula for a comparison of the $t^{4/3}$ -FP-evolution and the $t^{2/3}$ -FRW-evolution where we neglect the cosmological constant for a first orientation. In the extreme case of a transition during the recombination era, $z_{\text{tr}} = z_{\text{rec}} = 1300$, one finds

$$d_A(z_{\text{rec}})\Big|_{\alpha=4/3} \approx 10.3 d_A(z_{\text{rec}})\Big|_{\alpha=2/3} \quad (89)$$

We conclude that for realistic redshifts $z_{\text{tr}} \ll z_{\text{rec}}$ the value of $d_A(z_{\text{rec}})$ is bounded above by about 10 times its value in standard cosmology.

As for $d_H^S(z_{\text{rec}})$, we recall that in any $(\Omega_{\text{M}0}, \Omega_{\Lambda0})$ -FRW model the sound horizon at redshift $z \gg \Omega_{\text{M}0}, \Omega_{\Lambda0}$ has proper radius

$$d_H^S(z) \approx \frac{2c_s^{\text{eff}}}{H_0\sqrt{\Omega_{\text{M}0}}} (1+z)^{-3/2} \quad (90)$$

where c_{eff} is an effective speed of sound. In the extended FP model, the FRW cosmology preceding the FP era is characterized by the densities $\tilde{\Omega}_{\text{M}0}$ and $\tilde{\Omega}_{\Lambda0}$ of Eqs.(69), (70). This allows us to compare $d_H^S(z_{\text{rec}})$ in the extended FP model to the corresponding value in the $\Omega_{\text{M}0} = 1, \alpha = 2/3$ FRW model:

$$d_H^S(z_{\text{rec}})\Big|_{\text{FP}} = \sqrt{1 + (1+z_{\text{tr}})^3} d_H^S(z_{\text{rec}})\Big|_{\alpha=2/3} \quad (91)$$

Combining (89) to (91) we observe that the increase of $d_A(z_{\text{rec}})$ certainly cannot compensate for the increase of $d_H^S(z_{\text{rec}})$ so as to keep $\Delta\theta_s$ unaltered if the square root in (91) is larger than 10.3. The condition $\sqrt{1 + (1+z_{\text{tr}})^3} < 10.3$ leads to an upper bound for the transition redshift:

$$z_{\text{tr}} < 3.7 \quad (92)$$

This is a remarkable order of magnitude. It indicates that the transition should have taken place at or after the era of structure formation. This conclusion is in accord with the picture

arising from the analysis of density perturbations [19]. The actual value of z_{tr} is much smaller probably. For a more precise estimate the details of the microphysics should be taken into account properly which is beyond the scope of the present paper.

VII. CONCLUSIONS

In this paper we used the SCP and HST data on high redshift type Ia supernovae and the radio source data from Gurvits et al. [28] in order to test the infrared fixed point model proposed recently [16]. It predicts a time dependent cosmological and Newton constant whose dynamics arises from an underlying renormalization group flow, and it leads to a characteristic $t^{4/3}$ -time dependence of the scale factor in the late Universe. The latter gives rise to a very particular distance-redshift relation which, in principle, can be verified or falsified using distant supernovae as standard candles and compact radio sources as standard rods.

The results of our investigation based upon the χ^2 test can be summarized by saying that the IRFP model performs at least as well as the best-fit FRW model in reproducing the supernova and radio source data. Moreover, contrary to FRW cosmologies, it has *no free parameters* and thus actually *explains* why Ω_M and Ω_Λ are of the same order today. In fact, in the flat case, they are predicted to be exactly equal ($\Omega_M = \Omega_\Lambda = 0.5$), today and at any time in the future.

In the space of all cosmologies with a power law expansion $a \propto t^\alpha$, it seems to be precisely the exponent $\alpha = 4/3$ predicted by the IRFP model which yields the best fit to the data.

In this paper we also extended the original IRFP model of [16] by matching the fixed point regime with a preceding FRW era. We found that the statistical quality of the currently available data is not sufficient in order to determine when the Universe entered the fixed point epoch. However, using a Monte Carlo simulation we saw that the data expected from the forthcoming SNAP mission can teach us something about the transition to the fixed point regime provided it happened late enough, at a redshift smaller than 0.5, say.

In conclusion we think that the fixed point model is a viable alternative to the quintessence scenarios and certainly deserves being studied further. In particular it would be interesting to compare in more detail its predictions for the microwave background radiation to the data. We hope to address this issue in a future publication.

Acknowledgements

We are very grateful to Ariel Goobar who has provided us with the SNOOC code for the Monte Carlo simulation. We would like to thank V. Antonuccio, G. Esposito, G. Jorjadze, C. Kiefer, C. Rubano, G. Weigt and C. Wetterich for very interesting discussions. A.B. also acknowledges the warm hospitality of the Physics Departments of the University of Napoli and of Mainz University, where part of this work was written. E.B. acknowledges the Astrophysical Observatory of Catania (OACt) for financial support. M.R. is grateful to the OACt for the very kind hospitality extended to him.

APPENDIX A

In this appendix we resume the analysis of the supernova data in terms of the IRFP model proper, using a different statistical method: median statistics and a Bayesian model selection criterion.

1. Median statistics

Median statistics [20, 21] is more easily implemented than the χ^2 analysis and also less demanding with respect to the assumptions about the data because uncertainties need not be normally distributed, and no prior knowledge of measurement errors is required.

According to median statistics, the operation of calculating the likelihood of a particular model boils down to counting: one simply enumerates how many supernovae are, say, brighter than expected. Now, the probability that, when no systematic errors are present, n out of 92 SNe are brighter than expected ($92 - n$ being, of course, fainter) is given by the standard binomial distribution $P(n, 92)$. As for the fixed point model proper (without a FRW epoch) and the data set of III A, this number is found to be to $n = 53$ which has binomial probability $P(53, 92) = 0.029$. For comparison, we report in Table III the same analysis for other models. Notice that, if a model contains one or more free parameters, in column 1 we refer to those regions in the parameter space where the binomial probability is maximum.

At first sight the IRFP model seems to perform rather poorly in comparison with the FRW models. However, it is important to understand that the figures in the last column

TABLE III: Binomial likelihood after 92 SNe. (For models with free parameters, the numbers pertain to those regions in parameter space where the probability is maximum.)

Model	Brighter	Fainter	Binomial likelihood
Fixed point model ($z_{\text{tr}} > z_{\text{max}}$)	53	39	0.03
Extended fixed point model ($z_{\text{tr}} < 0.01$)	46	46	0.08
FRW with $\Omega_{\Lambda 0} = 0$, $0 \leq \Omega_{M0} \leq 0.1$	40	52	0.04
FRW with $\Omega_{\Lambda 0} + \Omega_{M0} = 1$, $0.4 \leq \Omega_{M0} \leq 0.5$	46	46	0.08
FRW with Ω_{M0} and $\Omega_{\Lambda 0}$ in the shaded region of Fig. 8	46	46	0.08

of Table III are not a measure for the correctness of the various models. In fact, the FRW models contain free parameters which always can be adjusted such that there is about the same number of brighter and fainter supernovae (at least if one allows for a cosmological constant). This is not possible with the IRFP model which contains no free parameters. Hence the naive median statistics is necessarily "unfair" towards the fixed point model. The correct way of assessing the "relative correctness" of the various models with their different number of free parameters is provided by Bayesian statistics, to which we shall turn in the next section.

2. Bayesian model selection

a. The method

In the Bayesian model selection the data set DS is assumed to have arisen from one of several possible models (or hypotheses) M_1, \dots, M_N . An a priori probability $P(M_i)$ is assigned to each model in order to measure the likelihood of M_i when no other information (e.g., observational) is available. This "prior" depends exclusively on the way each model is structured: we shall see below how to relate this number to the number of free parameters it presents. Let $P(DS|M_i)$ be the likelihood that a data set DS , such as the one that is actually observed, is attributable to M_i . Then, following Bayes' theorem, the posterior

probability $P(M_i|DS)$ that the model M_i is responsible for the observed data set DS is

$$P(M_i|DS) = \frac{P(DS|M_i) P(M_i)}{\sum_j P(DS|M_j) P(M_j)} \quad (\text{A1})$$

The likelihood $P(DS|M_i)$ equals the statistical probability that, given M_i is true, a set of n observations would result in the measured outcome DS . Therefore, these numbers are just the experimentally determined binomial probabilities that we have already discussed in section A 1.

b. Assigning a priori probabilities

Let us now assume we are trying to determine the “degree of belief” $P(M_i)$ that model M_i is the correct one, *before* we know anything about the way it reproduces observations. Apart from the constraint that

$$\sum_{i=1}^N P(M_i) = 1 \quad (\text{A2})$$

we have no other clues. Basically, we would like to quantify the extent to which a given model is constructed on an *ad hoc* basis. According to Ockham’s razor principle, the less free parameters are present, the more a model can be regarded as physically plausible. Bayesian priors can effectively help implementing this principle if one relates the initial probabilities $P(M_i)$ of a model to the number of free parameters it contains. Following [20], we then set

$$P(M_i) = \frac{1}{2^{N_i+1}} \quad (\text{A3})$$

where N_i is the number of free parameters of M_i . It is easy to see that this definition guarantees (A2), provided we share the corresponding probability into equal parts whenever there is more than one model with the same N_i .

In this paper we consider the following hypotheses:

1. M_1 : The IRFP cosmology correctly describes the cosmic evolution for $z < z_{\text{tr}}$, with $z_{\text{tr}} > z_{\text{max}}$;
2. M_2 : The Universe is described by a zero- Λ FRW cosmology, with $\Omega_{M0} > 0.1$;
3. M_3 : The Universe is described by a flat FRW model, with $0.4 \leq \Omega_{M0} \leq 0.5$;

4. M_4 : The Universe is described by a general FRW model, with Ω_{M0} and $\Omega_{\Lambda0}$ both in the shaded confidence region indicated in Fig. 8.

The number of free parameters and the corresponding priors are listed in Table IV. (Here and in the following “region 1” stands for the shaded region in Fig. 8 where the binomial probability is maximum.) The priors do not add up to unity yet; we shall comment on this point in a moment.

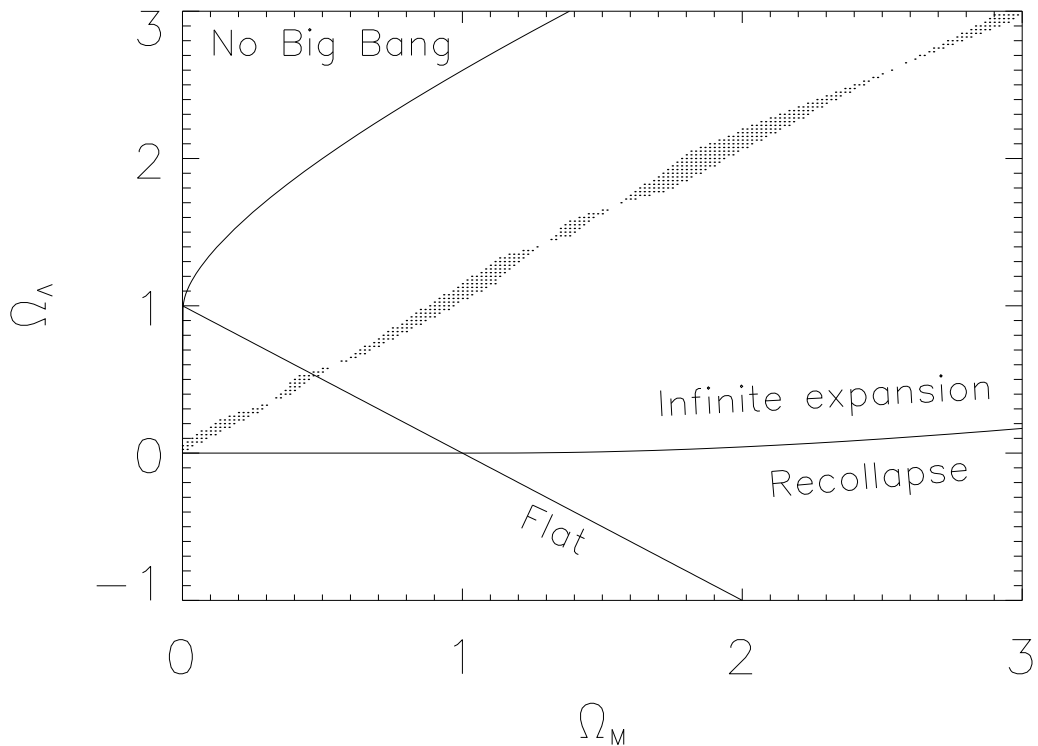


FIG. 8: FRW cosmology: the values of $(\Omega_{M0}, \Omega_{\Lambda0})$ in the shaded region maximize the binomial probability.

c. Comparison

We are now in a position to evaluate the final probability to affix to each model M_i as the “degree of belief” that, taking into account all the information in our possession, the hypothesis M_i is true. All we have to do is to take each prior $P(M_i)$ listed in Table

TABLE IV: Bayesian priors.

Model	Free parameters	Prior
Fixed point model ($z_{\text{tr}} > z_{\text{max}}$)	none	1/2
Extended fixed point model	1	1/12
FRW with $\Omega_{\Lambda 0} = 0$	1	1/12
FRW with $\Omega_{\Lambda 0} + \Omega_{M0} = 1$	1	1/12
FRW with Ω_{M0} and $\Omega_{\Lambda 0}$ in region 1	2	1/8

IV, multiply it by the measured binomial likelihood $P(DS|M_i)$ in Table III, calculate the normalization factor $\mathcal{N} \equiv \sum_i P(DS|M_i)P(M_i)$, and eventually compute the final probability $P(M_i|DS)$ according to (A1).

Our results are summarized in Table V. The fixed point model is found to perform better than any standard cosmology. It has a posterior probability of 37.5%, while the best-fit FRW model achieves only 25%. Clearly these two numbers are not too different, but probably it is safe to say that the fixed point model is at least as likely to be the correct theory of the late Universe as is the best standard cosmology. Also it should be kept in mind that the Bayesian result always depends on the choice for the priors. While our choice seems natural and has been used already in similar applications [20] it is clear that others are conceivable as well.

Please note that the numbers in the last column of Table IV do not add up to unity

TABLE V: Final probabilities.

Model	Confidence model is true (after 92 SNe Ia)
Fixed point model ($z_{\text{tr}} > z_{\text{max}}$)	0.36
Extended fixed point model	0.16
FRW with $\Omega_{\Lambda 0} = 0$	0.08
FRW with $\Omega_{\Lambda 0} + \Omega_{M0} = 1$	0.16
FRW with Ω_{M0} and $\Omega_{\Lambda 0}$ in region 1	0.24

yet. This is because we allow for models with more than 2 free parameters, whose prior probabilities, added up in the usual manner, $\sum_{N_i=3}^{+\infty} P(M_i)$, cooperatively make up for the missing 1/8. However, we can safely ignore these cosmologies in the calculation of the final probabilities, because they are strongly penalized by their small priors, $1/2^{N_i+1}$ with $N_i > 2$, and their inclusion in the computation does not significantly alter the results.

We can give a quantitative estimate of this assertion as follows: let us include in our discussion more and more cosmological models, M_i ($i = 5, \dots$), each characterized by N_i free parameters, with $N_i > 2$. Their priors $P(M_i)$ are certainly such that

$$P(M_i) \leq \frac{1}{16} \quad (i > 4) \quad (\text{A4})$$

On the other hand, their experimentally determined probabilities $P(DS|M_i)$ are subject to an upper bound, too, because they cannot exceed the maximum of the binomial likelihood function $P(n, 92)$, which is obtained for $n = 46$:

$$P(DS|M_i) \leq P(46, 92) = 0.08 \quad (\text{A5})$$

The increment in the normalization factor $\mathcal{N} = \sum_i P(DS|M_i)P(M_i)$, due to the new inclusions, is rather irrelevant:

$$\delta\mathcal{N} = \sum_{i=6}^{+\infty} P(DS|M_i)P(M_i) \leq 0.08 \sum_{i=6}^{+\infty} P(M_i) = 0.08 \sum_{N_i=3}^{+\infty} \frac{1}{2^{N_i+1}} = 0.01 \quad (\text{A6})$$

The value of \mathcal{N} , for the first 5 models only, amounts to 0.042. Therefore, the effect of including all the possible cosmologies with $N_i > 2$ is a shift of the value of \mathcal{N} from 0.042 to (at most) 0.052.

By eq. (A1), we also need to recompute the final probabilities $P(M_i|DS)$. For the first 5 models, we have:

$$P^{\text{new}}(M_i|DS) = \frac{P(DS|M_i)P(M_i)}{\mathcal{N} + \delta\mathcal{N}} = P^{\text{old}}(M_i|DS) \frac{\mathcal{N}}{\mathcal{N} + \delta\mathcal{N}} \quad (\text{A7})$$

Since

$$0 \leq \delta\mathcal{N} \leq 0.01 \quad (\text{A8})$$

the change in the final probabilities in Table V reduces to a simple rescaling by a factor that satisfies

$$0.81 \lesssim \frac{P^{\text{new}}(M_i|DS)}{P^{\text{old}}(M_i|DS)} \leq 1 \quad (\text{A9})$$

In particular, we observe that, irrespective of what the new models are (as long as $N_i > 2$, of course) or how well they compare to the data, the IRFP model will always have

$$P^{\text{new}}(M_1|DS) \gtrsim 29\% \quad (\text{A10})$$

We might wonder how this figure compares to the new final probabilities for the other cosmologies. As for the four models with $N_i \leq 2$, since $P^{\text{old}}(M_1|DS) > P^{\text{old}}(M_i|DS)$, $i = 2, 3, 4, 5$, eq. (A7) shows that

$$P^{\text{new}}(M_1|DS) > P^{\text{new}}(M_i|DS) \quad (\text{A11})$$

in all cases. (The final probabilities are merely scaled, so their ratios remain unchanged.)

As a last step, we must make sure that some of the new models do not acquire a final probability which is larger than $P^{\text{new}}(M_1|DS)$. This possibility is easily ruled out by using (A4), (A5) and (A8):

$$P^{\text{new}}(M_i|DS) = \frac{P(DS|M_i)P(M_i)}{\mathcal{N} + \delta\mathcal{N}} \leq \frac{0.08 \cdot \frac{1}{16}}{0.052} = 0.096 \quad (i = 6, \dots) \quad (\text{A12})$$

Therefore, the new models cannot achieve a confidence level of more than $\sim 10\%$. This upper bound is based entirely on the fact that they contain a number of parameters which is larger than 2. Our final figures, reported in Table V, reflect precisely these considerations, which fully entitle us to ignore any model with $N_i > 2$.

-
- [1] M. Carfora, K. Pietrkowska, Phys.Rev. D53 (1995) 4393; T. Buchert, M. Carfora, gr-qc/0101070; T. Buchert, M. Carfora, gr-qc/0210045;
 - [2] J.A. Belinchon, T. Harko, M.K. Mak, Class.Quant.Grav. 19 (2002) 3003 and gr-qc/0108074, and references therein.
 - [3] For a review see: J. Berges, N. Tetradis, C. Wetterich, hep-ph/0005122; C. Wetterich, hep-ph/0101178.
 - [4] M. Reuter, Phys.Rev. D57 (1998) 971 and hep-th/9605030.
 - [5] For a brief introduction see: M. Reuter in *Annual Report 2000 of the International School in Physics and Mathematics, Tbilisi, Georgia* and hep-th/0012069.
 - [6] O. Lauscher, M. Reuter, Phys.Rev. D65 (2001) 025013 and hep-th/0108040.

- [7] O. Lauscher, M. Reuter, *Class.Quant.Grav.* 19 (2002) 483 and hep-th/0110021; *Phys.Rev.* D66 (2002) 025026 and hep-th/0205062; *Int.J.Mod.Phys.* A17 (2002) 993 and hep-th/0112089.
- [8] M. Reuter, F. Saueressig, *Phys.Rev.* D65 (2002) 065016 and hep-th/0110054; *Phys.Rev.* D66 (2002) 125001 and hep-th/0206145.
- [9] R. Percacci, D. Perini, hep-th/0207033; D. Dou, R. Percacci, *Class.Quant.Grav.* 15 (1998) 3449.
- [10] W. Souma, *Prog.Theor.Phys.* 102 (1999) 181.
- [11] For a recent discussion of the UV fixed point within the 2 Killing vector reduction of QEG see: P. Forgács and M. Niedermaier, hep-th/0207028; M. Niedermaier, hep-th/0207143.
- [12] A. Bonanno, M. Reuter, *Phys.Rev.* D65 (2002) 043508 and hep-th/0106133.
- [13] M. Reuter, C. Wetterich, *Phys.Lett.* B188 (1987) 38.
- [14] A. Bonanno, M. Reuter, *Phys.Rev.* D62 (2000) 043008 and hep-th/0002196.
- [15] A. Bonanno, M. Reuter, *Phys.Rev.* D60 (1999) 084011 and gr-qc/9811026.
- [16] A. Bonanno, M. Reuter, *Phys.Lett.* B527 (2002) 9 and astro-ph/0106468.
- [17] V. Sahni, A. Starobinsky, astro-ph/9904398; N. Straumann, astro-ph/9908342.
- [18] For earlier work in this direction, see
N.C. Tsamis, R.P. Woodard, *Phys.Lett.* B301 (1993) 351; *Ann.Phys.* (NY) 238 (1995) 1;
I. Antoniadis, E. Mottola, *Phys.Rev.* D45 (1992) 2013;
I. Antoniadis, P. Mazur, E. Mottola, *Phys.Lett.* B444 (1998) 284.
- [19] A. Bonanno, M. Reuter, astro-ph/0210472, to appear on IJMPD.
- [20] J.R. Gott et al., *Ap.J.* 549 (2001) 1.
- [21] P.P. Avelino et al., *Astrophys.J.* 575 (2002) 989
- [22] S. Perlmutter et al., *Astrophys.J.* 517 (1999) 565.
- [23] A. Riess et al., *Astron.J.* 117 (1999) 707.
- [24] For a similar cosmology in a Brans-Dicke framework see
O. Bertolami, P.J. Martins, *Phys.Rev.* D61 (2000) 064007.
- [25] M. Reuter, C. Wetterich, *Nucl.Phys.* B506 (1997) 483;
A. Chamseddine, M. Reuter, *Nucl.Phys.* B317 (1989) 757.
- [26] Hamuy et al., *Astrophys.J.* 109 (1995) 1.
- [27] A. Goobar, E. Mörtzell, R. Amanullah, M. Goliath, L. Bergström, T. Dahlen, *Astron. & Astrophys.* 392 (2002) 757.

- [28] L.I. Gurvits, K.I. Kellermann, S. Frey, *Astron. Astrophys.* 342 (1999) 378.
- [29] D. Jain, A. Dev, J.S. Alcaniz, astro-ph/0302025.
- [30] Z. Zhu, M. Fujimoto, *Ap.J.* 581 (2002) 1.
- [31] D. Kalligas, P. Wesson, C.W.F. Everitt, *Gen.Rel.Grav.* 24 (1992) 351. See also:
A. Beesham, *Nuovo Cimento* 96B (1986) 17, *Int.J.Theor.Phys.* 25 (1986) 1295;
A.-M.M. Abdel-Rahman, *Gen.Rel.Grav.* 22 (1990) 655;
M.S. Berman, *Phys.Rev.* D43 (1991) 1075, *Gen.Rel.Grav.* 23 (1991) 465;
R.F. Sistero, *Gen.Rel.Grav.* 23 (1991) 1265;
T. Singh, A. Beesham, *Gen.Rel.Grav.* 32 (2000) 607;
A. Arbab, A. Beesham, *Gen.Rel.Grav.* 32 (2000) 615; A. Arbab, gr-qc/9909044.
- [32] C. Bennet et al., *Ap.J.*, in press, and astro-ph/0302207.
- [33] S. Weinberg, *Phys.Rev.* D64 (2001) 123511.
- [34] L. Knox, N. Christensen, C. Skordis, *Ap.J.* 581 (2001) L95.